Ocean Engineering 188 (2019) 106300

Contents lists available at ScienceDirect

Ocean Engineering

journal homepage: www.elsevier.com/locate/oceaneng

Prediction of short-term wind and wave conditions for marine operations using a multi-step-ahead decomposition-ANFIS model and quantification of its uncertainty

Mengning Wu [a,*], Christos Stefanakos [b], Zhen Gao [a,c,d], Sverre Haver [a,e]

[a] Department of Marine Technology, Norwegian University of Science and Technology (NTNU), Trondheim, NO-7491, Norway
[b] SINTEF Ocean, Department of Environment and New Resources, Trondheim, NO-7465, Norway
[c] Centre for Autonomous Marine Operations and Systems (AMOS), NTNU, Trondheim, NO-7491, Norway
[d] Centre for Marine Operations in Virtual Environments (MOVE), NTNU, Trondheim, NO-7491, Norway
[e] Department of Mechanical and Structural Engineering and Materials Science, University of Stavanger, Stavanger, NO-4036, Norway

ARTICLE INFO

Keywords:
Marine operations
Weather forecast
Multi-step-ahead prediction model
Uncertainty quantification

ABSTRACT

Short-term predictions of wind and wave properties with a duration of 1–3 days are vital for decision-making during the execution of marine operations. One-step-ahead weather conditions can be accurately predicted via various methods. However, prediction over long horizons is challenging since multi-step-ahead prediction is typically faced with growing uncertainties. In this study, a hybrid method for predicting multi-step-ahead wind and wave conditions is proposed, which combines a decomposition technique and the adaptive-network-based fuzzy inference system (ANFIS). First, the decomposition technique is applied to obtain stationary time series. Then, multi-step-ahead forecasting is conducted using ANFIS, in which three multi-step-ahead models (the M-1, M-N and M-1 slope models) are employed. To quantify the forecast uncertainty, the mean value and standard deviation of the error factor are calculated. The proposed method is evaluated by multi-step-ahead predictions within 24 h of wind and wave conditions at the North Sea center utilizing hourly time series of the mean wind speed U_w, the significant wave height H_s and the spectral peak period T_p. The results demonstrate that the forecast uncertainty increases with the prediction horizon, and a prediction range determined by the error factor provides a basic reference for the use of predicted environmental conditions for marine operations.

1. Introduction

According to the definition in Det Norske Veritas (2011), marine operations are non-routine operations of limited duration for handling objects and vessels in the marine environment during temporary phases, such as the transport of large offshore oil & gas platforms or topside structures, the installation of offshore platforms and offshore wind turbines, and the installation of subsea templates or structures. Such operations can only be performed within sea state limits. Weather statistics are used for planning operations while weather forecasts are required for deciding on when to start the operations. As a result, the accuracy of wind and wave condition forecasting is a critical factor in the planning of an operation during the execution phase. If the forecasted weather conditions are unsuitable for a marine operation, the operation will not be executed until the weather becomes suitable. However, if the actual future weather is within the safe limit, the opportunity for executing the marine operation will be wasted and the duration of the operation will be extended. By contrast, if the forecasted weather conditions are suitable for operation while the actual weather conditions are unsuitable during the operation window, the execution of the operation may lead to accidents such as injuries of personnel and damage to equipment.

However, in the prediction of weather conditions, several challenges are encountered, such as the random and unsteady characteristics of wind and waves. To predict environmental conditions accurately, various methods have been proposed by researchers, which can be classified into three main types: physical methods, statistical methods and machine learning methods. The physical methods consider meteorological parameters and physical laws in establishing physical models for weather condition forecasting. Among them, the use of empirical-based models in wave and wind forecasting is widespread. In

* Corresponding author.
E-mail address: mengning.wu@ntnu.no (M. Wu).

https://doi.org/10.1016/j.oceaneng.2019.106300
Received 30 May 2019; Received in revised form 8 August 2019; Accepted 9 August 2019
Available online 26 August 2019

empirical-based models, the generation of waves is assumed to be described by a function of meteorological parameters such as the fetch length and wind speed (Kazeminezhad et al., 2005). The most popular of such models are SMB (Bretschneider, 1970), Wilson (1965), JONSWAP (Hasselmann et al., 1973) and Donelan (1980). Although the empirical-based models are fast and accurate, they can only be applied in limited cases (Bishop, 1983; Kamranzad et al., 2011). With the rapid developments in computer technology, during the last two decades, several types of numerical models have been employed to forecast wave and wind characteristics. To predict wind characteristics such as the wind speed, numerical weather prediction (NWP) has been widely adopted (Cassola and Burlando, 2012; Landberg, 1999; Watson et al., 1994). The NWP model describes the physical processes of the atmosphere via conservation equations. By numerically solving the equations in terms of weather data such as the temperatures, pressure, surface roughness and obstacles, the wind speed can be predicted. Correspondingly, NWP requires abundant physical background knowledge and relatively long computation time (Foley et al., 2012; Landberg et al., 2003; Wang et al., 2016). In addition, various problems are encountered, such as lack of sufficient understanding for representing many physical processes in equation format and uncertainties in the surface characteristics, lateral boundary conditions and initial state (Al-Yahyai et al., 2010), which limit its practical application. For wave characteristic prediction, the most popular models are WAM (Group, 1988), Wave Watch III (Tolman, 1991) and SWAN (Booij et al., 1999). These models represent the sea state and predict the evolution of the wave spectrum based on the energy balance equation in space and time via numerical techniques. These techniques generally require expertise in their implementation (Browne et al., 2007; Mahjoobi et al., 2008).

In addition, data-driven approaches have been developed in recent years. Instead of considering physical phenomena in the environment, the data-driven approaches are purely mathematical and can predict wave and wind conditions based on only historical data. These approaches can be divided into two main categories: statistical methods and machine learning methods. The statistical methods express the future data as a linear or non-linear function of the historical data. The most popular and widely known statistical methods that are applied in wave and wind forecasting are the autoregressive model (AR) (Poggi et al., 2003; Schlink and Tetzlaff, 1998), the autoregressive moving average (ARMA) (Erdem and Shi, 2011; Lydia et al., 2016; Torres et al., 2005), the autoregressive integrated moving average (ARIMA) (Kamal and Jafri, 1997; Kavasseri and Seetharaman, 2009), and Kalman filter methods (Zuluaga et al., 2015). However, these methods typically cannot deal with non-linear patterns (Qin et al., 2017). By contrast, machine learning models consider a network that represents the relationship between inputs and outputs based on various algorithms and utilize this network to perform wave and wind forecasting. Models of this type can be applied to systems in which the interrelations are not clear. They can identify the relationship between the inputs and the outputs by learning from a large amount of data without relying on physical phenomena (such as diffraction, reflection, and wave breaking for computing wave reflection and diffraction or the wave spectrum and energy balance equation). Because of this advantage, representative machine learning techniques have been used for weather forecasting, such as support vector machine (SVM) (Berbić et al., 2017; Kamranzad et al., 2011; Mahjoobi and Mosabbeb, 2009), artificial neural networks (ANNs) (Agrawal and Deo, 2002; Chang et al., 2017; Deo et al., 2001; Jain and Deo, 2007; Mandal et al., 2005) and the fuzzy inference system (FIS) (Kazeminezhad et al., 2005; Özger and Şen, 2007). The adaptive-network-based fuzzy inference system (ANFIS), which is a hybrid intelligent system (a combination of ANN and FIS), has been employed recently. Özger and Şen (2007) and Akpınar et al. (2014) applied ANFIS to predict wave parameters and compared the auto-regressive moving average results with the results of the exogenous input (ARMAX), Wilson, Shore Protection Manual (SPM), JONSWAP, and Coastal Engineering Manual (CEM) methods. Kazeminezhad et al. (2007) compared wave predictions that were obtained via ANFIS with those of other methods, such as the CEM, ANN and FIS methods. In addition, the efficiencies of ANFIS, support vector machines (SVMs), Bayesian networks (BNs), and ANNs in wave height prediction were investigated by Malekmohamadi et al. (2011). In most of the above studies, historical data were used directly to train ANFIS model; thus, the non-stationarity of the data was ignored. Stefanakos and Schinas (2015) and Duru and Yoshida (2012) conducted a series of studies and proved that non-stationarity is inherent in time series of wind and wave parameters due to the seasonal effect. Therefore, prior to forecasting, the non-stationarity should be removed from the initial time series. Based on this strategy, Stefanakos (Stefanakos, 2016a, b; Stefanakos and Vanem, 2018) developed an ANFIS model via non-stationary modelling for the prediction of wind and wave parameters at the North Atlantic and the Pacific Ocean, and more accurate forecasts were obtained.

These studies consider only one-step-ahead prediction; approaches for generating multi-step-ahead forecasts have rarely been studied because compared to one-step-ahead forecasting, multi-step-ahead prediction is more difficult (Taieb and Bontempi, 2011) since growing uncertainties due to, e.g., lack of information and accumulation of prediction errors, must be considered. However, an advantage of multi-step-ahead wind and wave forecasting is that it can provide more information about the future, which is important for marine operations as weather variations in the future are a critical factor in decision-making during the execution of marine operations. Deo and Naidu (1998) used neural networks to predict ocean wave heights in real time. In that study, one-to two-step-ahead predictions were obtained based on the current observations and according to the simulations, the forecasting accuracy decreased as the forecasting lead time increased. Basu et al. (2005) developed a nonlinear technique that was based on the genetic algorithm (GA) for significant wave height prediction. In that work, daily time series of the surface wind speed and the significant wave height in the Arabian Sea and the Bay of Bengal were used to develop the technique and three-step-ahead prediction was conducted. Ahmed and Khalid (2017) presented a nonlinear autoregressive neural network (NARNN) for predicting wind speed up to six hours ahead. Niu et al. (2018) proposed a hybrid approach for 1-step-, 3-step- and 6-step-ahead wind speed forecasting that utilized optimal feature selection and an ANN. All results demonstrated that the forecast error increased significantly with each step-ahead forecast.

Although the above studies consider the application of multi-step-ahead prediction models, they focus on forecasting up to six steps in the future; few studies have considered prediction with more steps ahead. Such forecasting is much more important in practice, especially for marine operations because some operations must be viewed as continuous events. Hence, once the first operation has been performed, the operation cannot be interrupted and the duration of the entire process will be more than just a few hours. Under this circumstance, multi-step-ahead prediction with larger numbers of steps ahead can effectively capture the dynamic behavior of future wave and wind conditions during the execution process, which is crucial for improving the security of entire marine operations. Based on this background, the main objective of this work is the development of a multi-step-ahead model for weather condition forecasting with a long forecast horizon.

Considering the data used (hourly time series of mean wind speed (U_w), significant wave height (H_s) and spectral peak period (T_p) from 2001 to 2010 at the North Sea center) and the timetable for marine operations, this work intends to predict wind and wave conditions in one day ahead, namely, twenty-four steps ahead. To realize multi-step-ahead predictions, a hybrid method consisting decomposition technique and ANFIS is developed. Firstly, the training and testing data are pre-processed by the decomposition technique. Then, the ANFIS combined with a multi-step ahead model (M-1, M-N or M-1 slope) is built based on the training data. The M-1 model applies a one-step prediction model iteratively, where the forecasted data are utilized as the input for the prediction of the following time step. The M-1 slope model also adopts

Fig. 1. North Sea area and the site locations.

forecasted data but includes slope information when selecting the training dataset. Instead of using forecasted data, the M-N model only applies the actual data and redevelops a new model for each time step. Furthermore, the forecast performance of the prediction model is evaluated on the testing data by an uncertainty quantification analysis of the forecast errors at each lead time. Finally, a method of applying the confidence interval for the predicted conditions is proposed, to utilize the long-horizon forecasts.

The remainder of this paper is organized as follows: Section 2 presents a brief description of the study site and the considered environmental data. In Section 3, the details of the methodology are introduced. The decomposition technique, ANFIS, multi-step-ahead forecasting models, uncertainty quantification analysis and the whole process are described in this section. Then, the short-term prediction of wind and wave conditions at the center of the North Sea is conducted in Section 4. Section 4.1 investigates the weather forecasting performance of the decomposition-ANFIS method in terms of the one-step-ahead prediction results. Section 4.2 selects the optimal multi-step-ahead models and performs a comparative analysis with the proposed models. Finally, the main conclusions of this study are summarized in

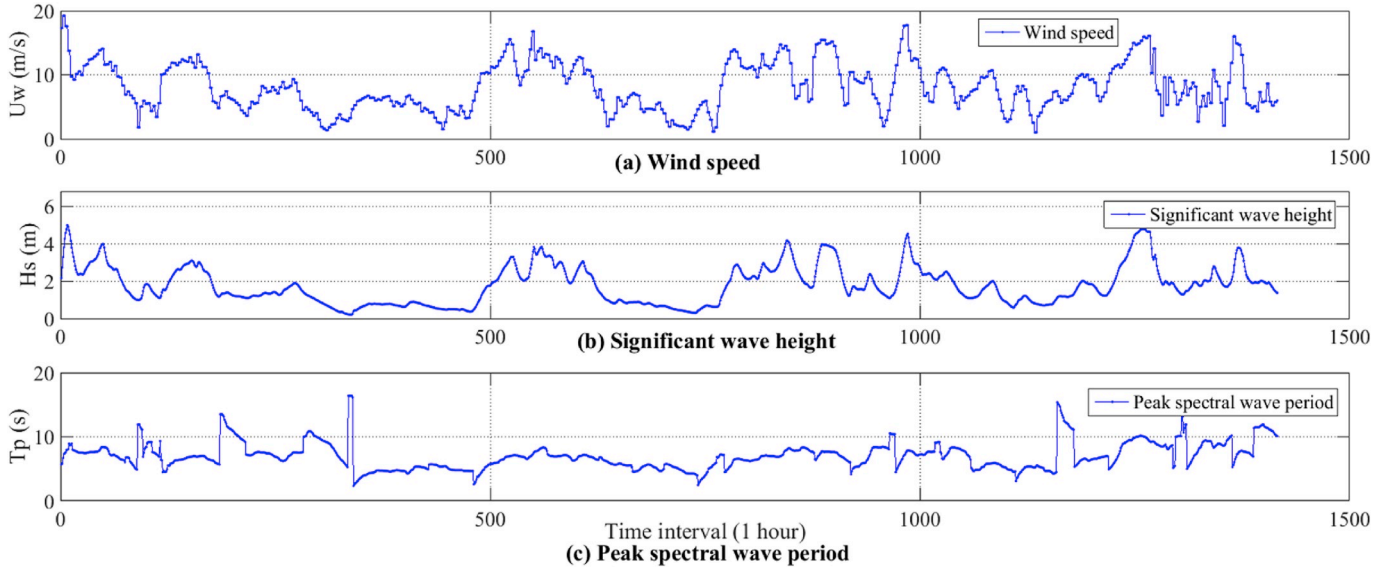

Fig. 2. Two-month time series of U_w, H_s and T_p for winter (2001.01.01–2001.02.28).

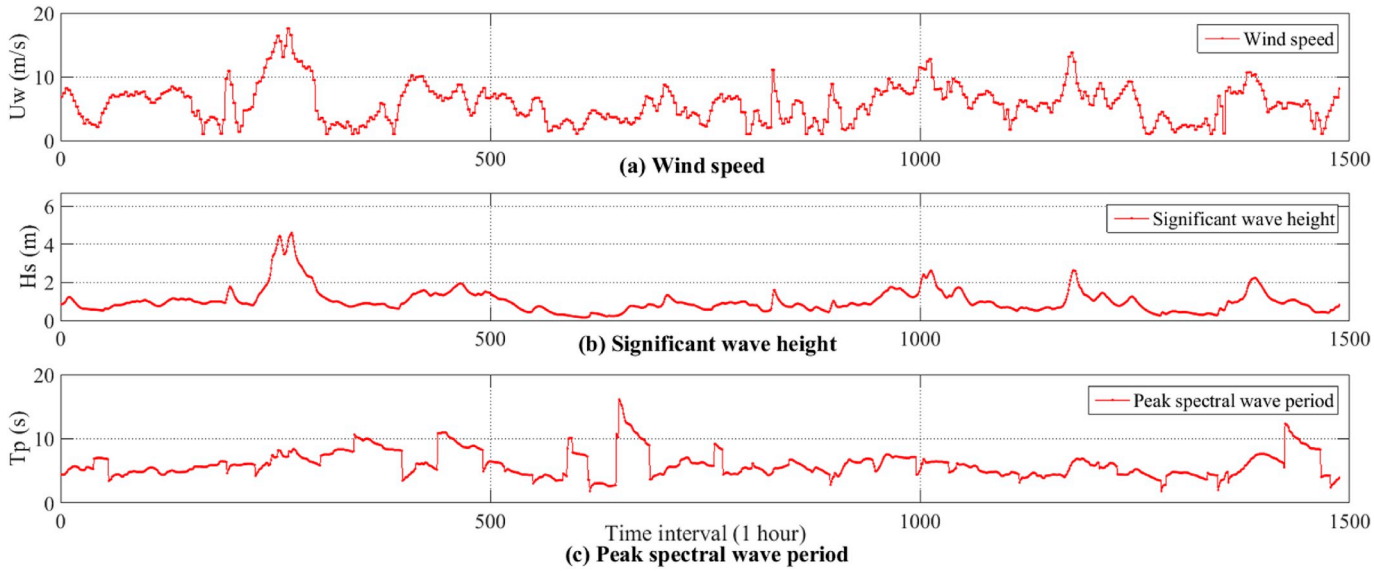

Fig. 3. Two-month time series of U_w, H_s and T_p for summer (2001.07.01–2001.08.31).

Section 5.

2. Offshore site and environmental data

In the application of the weather conditions to marine operations, the environmental variables that typically must be forecasted are the mean wind speed U_w, the significant wave height H_s and the peak spectral wave period T_p. In this study, the North Sea is considered and 18 sites in this area are illustrated in Fig. 1. The dataset in each site is comprised of hindcast data that are based on a high-resolution regional atmospheric model (SKIRON) and an ocean wave model (WAM). To generate the hindcast data, the mean wind speed at a height of 10 m above the mean sea level is produced by the atmospheric model. Then, it will be used as the input for the wave model to obtain wave properties. Based on these properties, three-hourly time series of the mean wind speed U_w and hourly time series of the significant wave height H_s and the peak spectral wave period T_p are obtained. The covered period is from January 2001 to December 2010. For additional details, see Li et al. (2013). Although these data are hindcast data, we consider them as actual data that will be used to generate the ANFIS model for prediction and for testing.

The North Sea Center (site 15, Fig. 1) is selected as the study site in this paper. Many marine operations such as the monopile installation (Acero et al., 2016) and blade installation (Jiang et al., 2018) of an offshore wind turbine have been designed and analyzed in this region. This site is a shallow shelf sea with a mean water depth of 29 m and a distance to shore of 300 km. During the specified period, the 50-year return period wind speed and the significant wave height are 27.2 m/s and 8.66 m, respectively, and the mean value of the peak spectral wave period is 6.93 s.

As an overview of the environment at this site, time series U_w, H_s and T_p of two months of winter from 2001.01.01 to 2001.02.28 (1416 hourly points) and those of summer from 2001.07.01 to 2001.08.31 (1488 hourly points) are presented in Figs. 2 and 3, respectively. High variability is observed in all three series in summer and winter. Therefore, it is necessary to predict environmental conditions prior to executing marine operations. However, in modelling multi-step-ahead prediction, significant challenges are encountered due to the randomness and non-stationarity of the time series. In such cases, to obtain predictions via forecasting methods, sufficient data must be used to train the model. Accordingly, in the ten-year hourly time series of U_w, H_s and T_p, the data for the first nine years (78888 data points) are selected as the training data and the data for the tenth year (8760 data points) are selected as the testing data, which is sufficiently long for investigating the behavior of forecast uncertainty in models with a possibility of covering most of the typical sea states.

3. Methodology

3.1. Decomposition technique

A long-term time series of wave or wind data can be considered as a nonlinear, non-stationary and seasonal time series. For data of this type, the monthly mean value and the standard deviation of the series can be used to extract the non-stationarity (Athanassoulis and Stefanakos, 1995). The object is extended to a multi-variate time series and the decomposition model (Stefanakos and Schinas, 2014) can be expressed as follows Eq. (1):

$$\underset{(N\times 1)}{Y(t)} = \underset{(N\times 1)}{M(t)} + \underset{(N\times N)}{\sum(t)} \underset{(N\times 1)}{W(t)} \tag{1}$$

or, in matrix notation,

$$\begin{bmatrix} Y_1(t) \\ Y_2(t) \\ \vdots \\ Y_n(t) \\ \vdots \\ Y_N(t) \end{bmatrix} = \begin{bmatrix} M_1(t) \\ M_2(t) \\ \vdots \\ M_n(t) \\ \vdots \\ M_N(t) \end{bmatrix} + \begin{bmatrix} \Sigma_{11}(t) & \Sigma_{12}(t) & \cdots & \Sigma_{1N}(t) \\ \Sigma_{21}(t) & \Sigma_{22}(t) & \cdots & \Sigma_{2N}(t) \\ \vdots & \vdots & \vdots & \vdots \\ \Sigma_{n1}(t) & \Sigma_{n2}(t) & \cdots & \Sigma_{nN}(t) \\ \vdots & \vdots & \vdots & \vdots \\ \Sigma_{N1}(t) & \Sigma_{N2}(t) & \cdots & \Sigma_{NN}(t) \end{bmatrix} \begin{bmatrix} W_1(t) \\ W_2(t) \\ \vdots \\ W_n(t) \\ \vdots \\ W_N(t) \end{bmatrix} \tag{2}$$

where the number of time series is N.

In Eq. (2), $\mathbf{Y}(t)$ represents the initial time series and it can be expressed as

$$\left\{ Y_n(j,\ m,\ \tau_k),\ \begin{matrix} j = 1, \cdots J \\ m = 1, \cdots, 12 \\ k = 1, \cdots, K_m \end{matrix} \right\},\quad n = 1, \cdots N \tag{3}$$

where j is the year index, m is the month index and τ_k is the kth observation in the mth month. The number of observations in the mth month

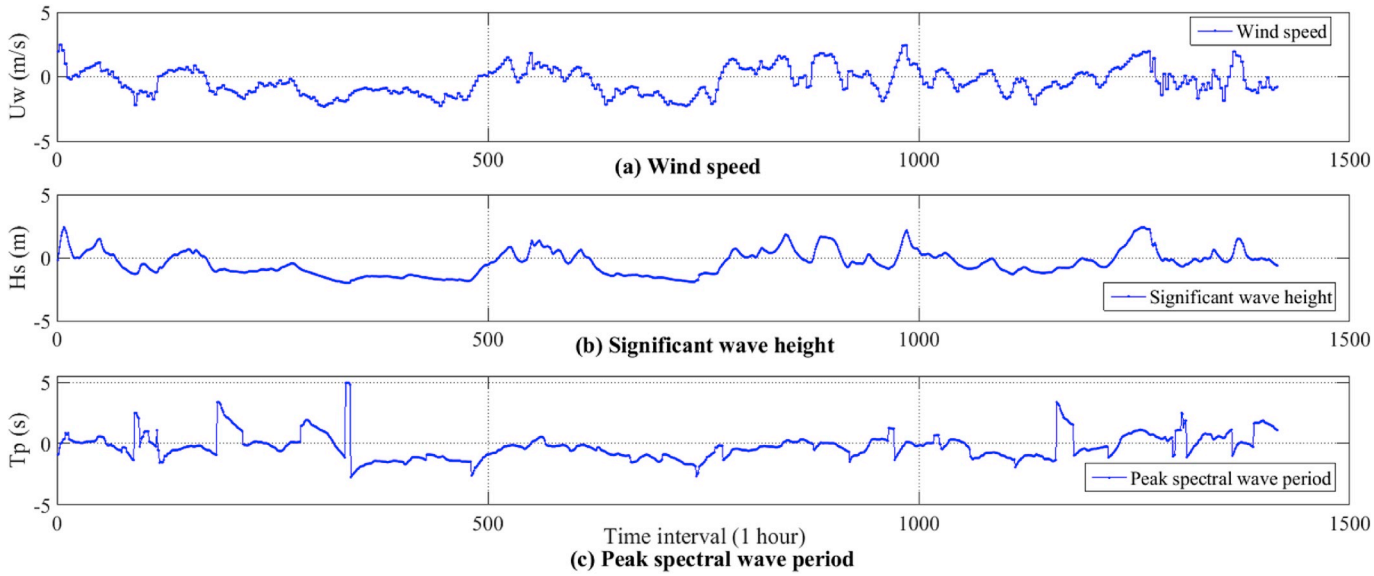

Fig. 4. Decomposed time series of U_w, H_s and T_p for winter (2001.01.01–2001.02.28).

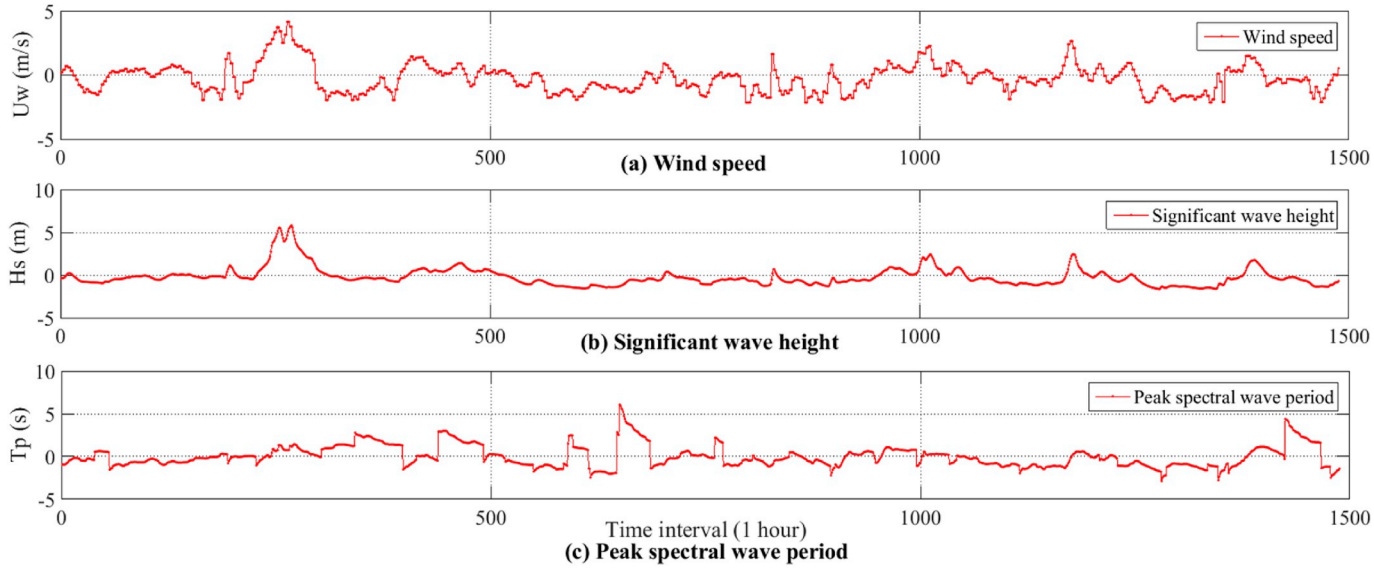

Fig. 5. Decomposed time series of U_w, H_s and T_p for summer (2001.07.01–2001.08.31).

is K_m.

The seasonal patterns are characterized by $\mathbf{M}(t)$ and $\mathbf{\Sigma}(t)$, which are the monthly mean value vector and the covariance matrix with period of one year, respectively. These two terms can be estimated by averaging the time series of monthly mean values $M_{3,n}(j,m)$ and the covariance matrix $S_{3,nl}(j,m)$ over J years (Stefanakos et al., 2006):

$$\tilde{M}_{3,n}(m) = \frac{1}{J}\sum_{j=1}^{J} M_{3,n}(j,m) = \frac{1}{J}\sum_{j=1}^{J}\frac{1}{K_m}\sum_{k=1}^{K_m} Y_n(j,\ m,\ \tau_k) \tag{4}$$

with $m = 1, 2, \ldots, 12$. The subscript '3' denotes that these two terms are statistics with respect to the third index in $Y_n(j,m,\tau_k)$.

Apart from the seasonal patterns, the residue part, namely, $\mathbf{W}(t)$, is the corresponding stationary time series of $\mathbf{Y}(t)$.

In this study, there are three initial joint long-term time series of wind and wave parameters (the mean wind speed U_w, the significant wave height H_s and the peak spectral wave period T_p), namely, N equals 3 in Eq. (3). Via Eqs. (4)-(5), the deterministic seasonal patterns, namely, $[\mathbf{M}(t), \mathbf{\Sigma}(t)]$, can be easily estimated from the data. After that, the corresponding stationary time series, namely, $\mathbf{W}(t)$, can be calculated via

$$\tilde{S}_{3,nl}(m) = \frac{1}{J}\sum_{j=1}^{J} S_{3,nl}(j,\ m) = \frac{1}{J}\sum_{j=1}^{J}\sqrt{\frac{1}{K_m}\sum_{k=1}^{K_m}\left[Y_n(j,\ m,\ \tau_k) - M_{3,n}(j,\ m)\right]\left[Y_l(j,\ m,\ \tau_k) - M_{3,l}(j,\ m)\right]},\quad n,l = 1,\cdots,N \tag{5}$$

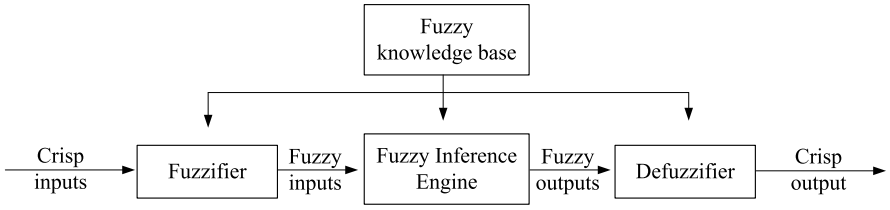

Fig. 6. Fuzzy inference system architecture.

1. Fuzzifier. It performs the fuzzification of the input variables into fuzzy inputs using the MFs that are stored in the fuzzy knowledge base.
2. Fuzzy knowledge base. It is composed of the data base and the rule base, which contain the MFs of the fuzzy sets and the IF-THEN rules, respectively.
3. Inference engine. It maps the set of fuzzy inputs to fuzzy outputs according to the IF-THEN rules.
4. Defuzzifier. It defuzzifies the fuzzy outputs into a crisp output.

Eq. (2). To demonstrate this clearly, the decomposed time series that correspond to the series in Figs. 2 and 3 are plotted in Figs. 4 and 5. The time series after decomposition are zero-mean stochastic processes and the seasonal effects in the data are significantly reduced.

3.2. ANFIS

The adaptive-network-based fuzzy inference system (ANFIS) (Jang et al., 1996) is a hybrid intelligent system that is a combination of a fuzzy inference system (FIS) and an adaptive neural network (ANN). First, the FIS is presented. A fuzzy inference system (FIS) is a nonlinear method for mapping inputs to output that is based on fuzzy logic theory. In fuzzy logic theory, the focus is on understanding the concept of a fuzzy set. In a class set, an element is either a member of the set or not and the corresponding result is 1 or 0. By contrast, a fuzzy set is a set that lacks a clearly defined boundary. A fuzzy set is an extension of a classical set whose elements can belong to more than one set and the membership degree, which is between 0 and 1, is used to quantify the grade of membership of the element to each set. The degree of membership of a set is defined by a membership function (MF), which provides a measure of the similarity of the element to a fuzzy set. For example, if X is a universe of discourse (such as H_s) and x is an element of X, then a fuzzy set O (such as 'High') on X can be described as Eq. (6):

$$O = \{(x, \mu_O(x)), \quad x \in X\} \tag{6}$$

where $\mu_O(x)$ is the membership function that is associated with x in fuzzy set O and expresses the degree to which a value of H_s belongs to set 'High'. The most common types of MFs are triangular, Gaussian, and sigmoid.

In a FIS, the mapping of input variables to an output is characterized by a list of fuzzy statements, which are called IF-THEN rules. IF-THEN rules are expressions of the form 'If x is A, then y is B' and are used to infer a fuzzy output based on fuzzy inputs, where A and B are linguistic labels of fuzzy sets characterized by MFs. The structure of a FIS is illustrated in Fig. 6 that consists of four functional blocks.

There are two important types of fuzzy inference methods: the Mamdani (1974) and Takagi-Sugeno (Takagi and Sugeno, 1993) fuzzy inference methods. They differ in terms of their defuzzification schemes and the latter is used in this study. In the TS method, the outcome of each IF-THEN fuzzy rule is a scalar value rather than a fuzzy set for the output

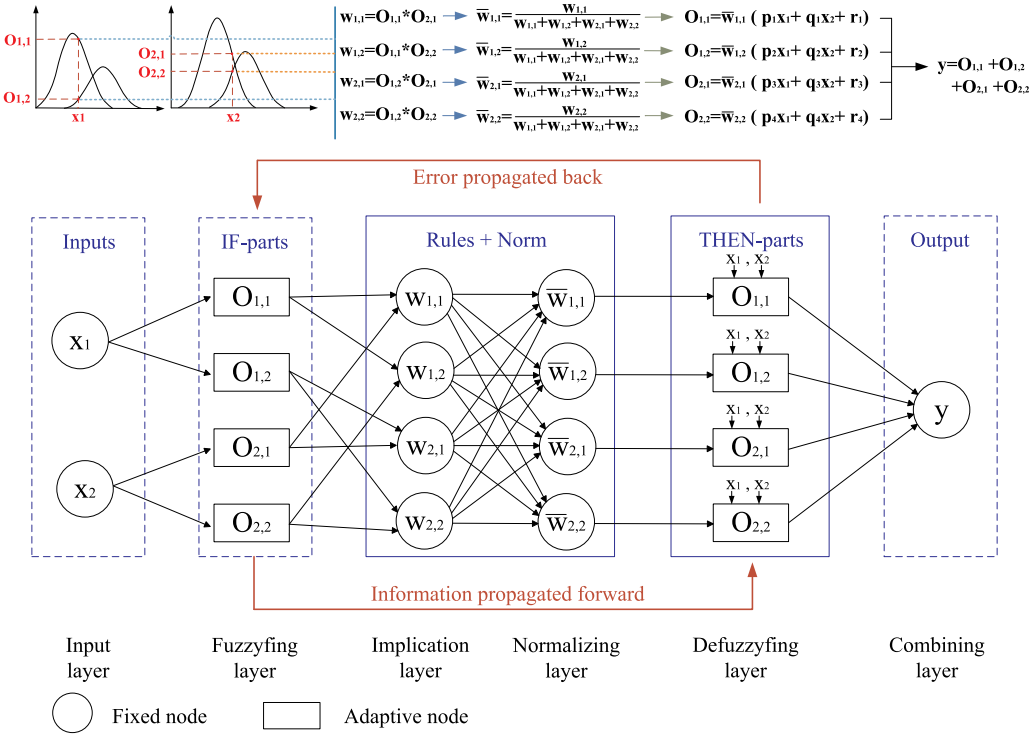

Fig. 7. ANFIS architecture.

variable of the form Eq. (7):

$$\text{IF} \quad x_1 \ is \ S_r^{(1)},\ x_2 \ is \ S_r^{(2)},\ \cdots,\quad x_n \ is \ S_r^{(n)}$$

$$\text{THEN} \quad y = p_r x_1 + q_r x_2 + \cdots + t_r x_n \tag{7}$$

where x_i and y are the inputs and output, respectively. $S_r^{(i)}$ is a linguistic value (such as 'low' or 'high' for H_s), which is represented by a fuzzy set, and p_r, q_r, and t_r are parameters that must be determined. The IF part is called the premise, which contains the MFs' parameters that describe the shapes of the MFs, and the THEN part is called the consequent, which contains parameters that describe the linear relationship of the inputs.

When using FIS, the main challenge is the selection of the parameters in the fuzzy knowledge base. Traditionally, the parameters are determined based on the experience of experts or past available data of the system. For selecting the parameters, an adaptive neural network is combined with the FIS to optimize the premise and consequent parameters based on the available datasets using a hybrid learning algorithm. This strategy was proposed by Jang (1993) and the method in which an adaptive neural network and FIS are combined is called the adaptive-network-based fuzzy inference system (ANFIS). In practice, the structure of ANFIS is similar to that of a multi-layer neural network. ANFIS has an input layer, an output layer and three hidden layers that are related to MFs and IF-THEN rules. To illustrate the procedure, the structure of a simple ANFIS that consists of two inputs, namely, x_1 and x_2, and one output, namely, y, is presented in Fig. 7.

In this ANFIS structure, the first layer is the input layer, which contains crisp inputs x_1 and x_2. The second layer is the fuzzifying layer, in which the inputs x_i are fuzzified into the membership values $\mu_{Aj}(x_i)$ based on the MFs of linguistic labels A_j, as expressed in Eq. (8). This layer can be considered an adaptive layer since the outputs depend on the parameters in the MFs. In this example, the MFs, which are denoted as μ_{Aj}, are Gaussian-type functions.

$$O_{i,j} = \mu_{A_j}(x_i), \quad for\ i,j = 1,2 \tag{8}$$

If the number of crisp inputs exceeds one, the weight of each rule must be determined by using fuzzy operators. The third layer contains two operators and is divided into two layers, which are called the implication and normalizing layers. In these two layers, the firing strength $w_{i,j}$ for each rule and the normalized firing strength $\overline{w}_{i,j}$ are calculated via Eqs. (9)-(10).

$$w_{i,j} = \mu_{A_i}(x_1) \times \mu_{A_j}(x_2), \quad for\ i,j = 1,2 \tag{9}$$

$$\overline{w}_{i,j} = \frac{w_{i,j}}{\sum w_{i,j}}, \quad for\ i,j = 1,2 \tag{10}$$

Then, the outcome $O_{i,j}$ of each rule can be calculated in the defuzzifying layer using the corresponding IF-THEN rule and the obtained rule's weight, as expressed in Eq. (11). Similarly, this layer is also an adaptive layer because parameters p_i, q_i and r_i in the IF-THEN rules should be determined.

$$O_{i,j} = \overline{w}_{i,j} \cdot y_{i,j} = \overline{w}_{i,j} \cdot (p_k x_1 + q_k x_2 + r_k), \quad for\ i,j = 1,2,\ \ k = 1,\ldots,i*j \tag{11}$$

Based on the sum of all outcomes $O_{i,j}$ (the weighted average of all IF-THEN rules' results), the overall output y can be estimated via Eq. (12).

$$y = \sum O_{i,j} \tag{12}$$

In this process, an adaptive neural network is applied to determine the parameters in the two adaptive layers, which is represented by the red cycle in Fig. 7. According to the fixed values of the premise parameters in the IF part, the information is propagated forward to identify the consequent parameters via the least-square method. In addition, by fixing the consequent parameters in the THEN part, the error is propagated back to the fuzzifying layer and the premise parameters are modified. Then, the optimal values can be tracked. By performing this procedure based on the training data, the optimal ANFIS can be identified. Overall, the only information that must be specified by the user is the number and the types of MFs for each input variable.

In this study, the ANFIS is utilized for both one- and multi-step-ahead predictions. For one-step-ahead prediction, three simplest ANFISs for the mean wind speed U_w, the significant wave height H_s and the spectral peak period T_p are developed, which are expressed in Eqs. (13)-(15), respectively. The basic idea is to use the training dataset to derive functional relationships between the parameters at the current time and at the next time step so that one-step-ahead prediction can be made. However, multi-step-ahead prediction requires more complex ANFIS models, which will be presented and discussed in Section 3.3. (a) Mean wind speed U_w:

$$U_w(t+1) = f_1(U_w(t)) \tag{13}$$

(b) Significant wave height H_s:

$$H_s(t+1) = f_2(U_w(t), H_s(t)) \tag{14}$$

(c) Peak spectral wave period T_p:

$$T_p(t+1) = f_3(U_w(t), H_s(t), T_p(t)) \tag{15}$$

where function f in each system represents the prediction model. The number of rules depends on the fuzzy sets for each input variable.

3.3. Multi-step-ahead forecasting models

For one-step-ahead prediction, only data at the current time are used as input to predict the next-step data, as expressed in Eqs. (13)-(15). However, due to the complexity of the prediction, applying the same model to multi-step-ahead forecasting will result in a significant reduction in accuracy. Therefore, several alternatives have been proposed for building multi-step-ahead prediction models. In Sections 3.3.1-3.3.3, three models for realizing multi-step-ahead forecasting are discussed in detail.

Every forecasting model requires more than one input. To maintain the consistency of the variables, data at any time t are represented by X (t). X(t + N) denotes the N-step-ahead data, which are unknown output, and (X(t), X(t-1), …, X(t-M+1)) represents the input set, which contains the previous M data. In addition, f denotes the prediction model between the inputs and the output.

3.3.1. M-1 model

The M-1 model requires only the training of a one-step-ahead prediction model f based on the training data, which is expressed as Eq. (16):

$$X(t+1) = f(X(t),\ X(t-1), X(t-2), \ldots,\ X(t-M+1)) \tag{16}$$

To forecast N steps ahead, the above model is applied iteratively. However, in the input set, the predicted value of the previous step is used instead of the actual data. Considering prediction of significant wave height H_s as an example, after establishing the one-step-ahead prediction model, one-step-ahead value $H_s(t+1)$ is predicted Eq. (17):

$$\widehat{H}_s(t+1) = f(H_s(t),\ H_s(t-1),\ H_s(t-2),\ \ldots,\ H_s(t-M+1)) \tag{17}$$

Then, the forecasted value, namely, $\widehat{H}_s(t+1)$, is considered as part of the input set for predicting the next-step value, namely, $\widehat{H}_s(t+2)$, based on the same one-step-ahead model f Eq. (18):

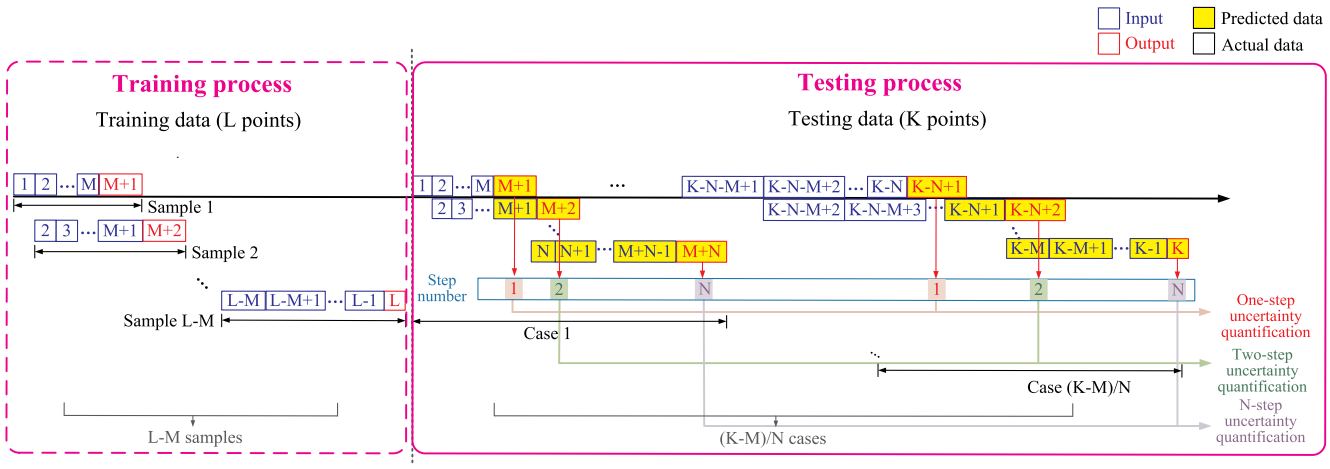

Fig. 8. Architecture of the M-1 multi-step-ahead prediction method.

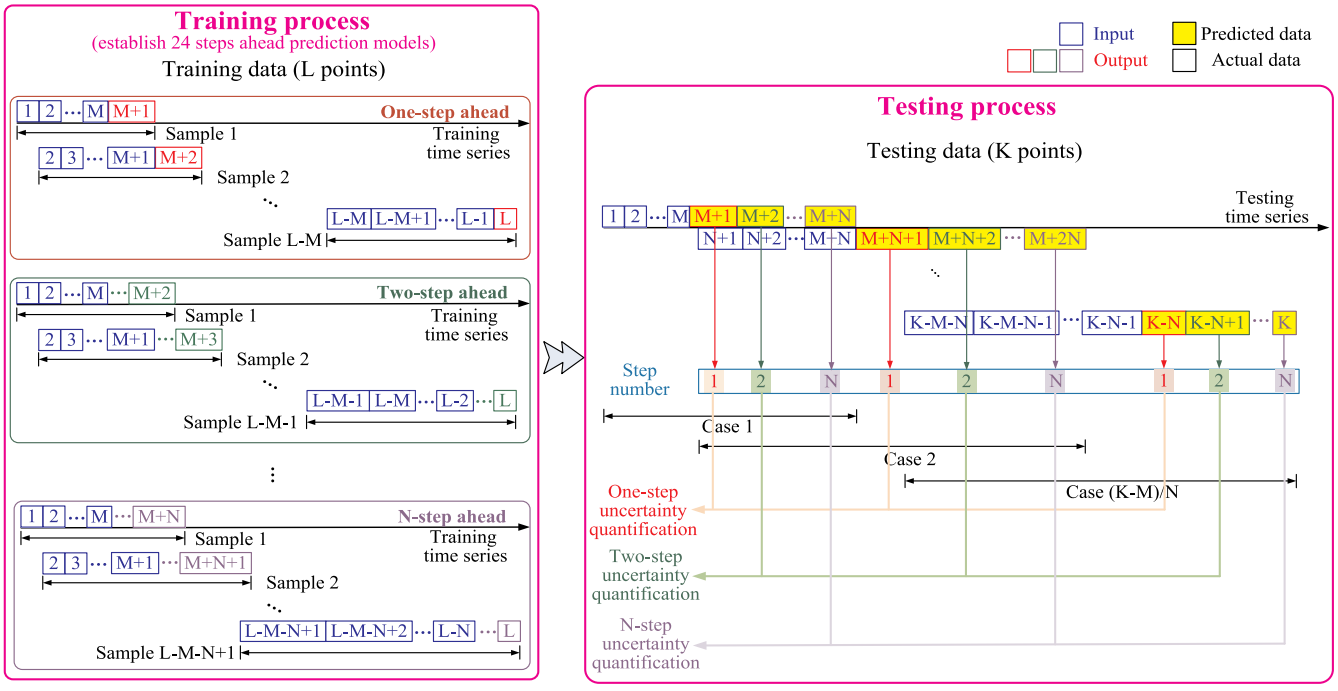

Fig. 9. Architecture of the M-N multi-step-ahead prediction method.

$$\hat{H}_s(t+2) = f(\hat{H}_s(t+1), H_s(t), H_s(t-1), H_s(t-2), \ldots, H_s(t-M+2)) \tag{18}$$

Then, for the N-step-ahead prediction, this procedure is repeated and $\hat{H}_s(t+3)$ to $\hat{H}_s(t+N)$ are predicted iteratively. The iteration process may lead to accumulated errors since after one-step prediction, the input set is composed of forecasted values rather than actual data. Especially when N exceeds M, namely, after M-step-ahead prediction, the input set does not contain any actual data, but only forecasted values. In such cases, the forecasts may suffer from low performance. However, the main advantage of the M-1 model is that only one training process is required for obtaining the prediction model and this model does not change between steps. Therefore, the forecasting time is significantly reduced and the computational efficiency is increased.

To illustrate the application of the M-1 model in this study, the architectures of both the training and testing processes are plotted in Fig. 8. In Fig. 8, it is assumed that the training and testing sets contain L and K points, respectively. To determine the optimal function, which is expressed in Eq. (16), L-M samples are used to train the relationship between the inputs and the output. The inputs and output are represented by blue and red boxes, respectively, in Fig. 8. Then, in the testing data set, for a specified input vector, the following N-step-ahead forecasts can be predicted directly via iteration under the established prediction model. The boxes that are highlighted in yellow represent the predicted data and as the number of steps increases, the number of predictions that are used as inputs to obtain the next-step forecast value also increases. A complete simulation of obtaining N-step-ahead predictions is considered one case. To evaluate the M-1 model, the prediction process is repeated over the testing period to obtain many forecast cases ((K-M)/N cases in this example). Then, the forecast uncertainty of the model at step one to step N can be evaluated via

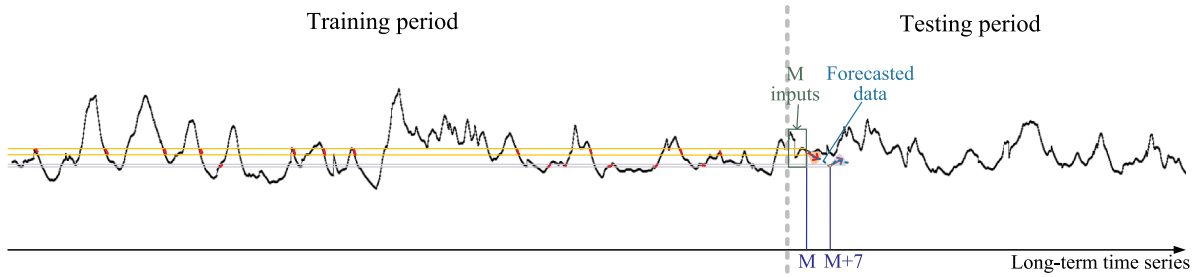

Fig. 10. Architecture of the M-1 slope multi-step-ahead prediction method.

uncertainty quantification analysis, which is described in Section 3.4.

3.3.2. M-N model

In the M-N model, a separate training process and the corresponding prediction model f_N are required at each step N. The prediction model can be represented as Eq. (19)

$$X(t+N) = f_N(X(t),\ X(t-1), X(t-2), \ldots,\ X(t-M+1)) \quad (19)$$

where f_N denotes the prediction model at step N.

In the M-N model, the input set always consists of the last M data in the time series that are known. Therefore, in contrast to the M-1 model, the M-N model does not use any predicted value and, thus, prevents accumulated errors. However, this model is time-consuming since N models must be trained independently when forecasting N steps ahead. Furthermore, the correlation between inputs and output weakens as N increases, thereby increasing the difficulty of capturing their relationship.

The architecture of the M-N model that is applied in this study is illustrated in Fig. 9. In the training process, N-step-ahead prediction models are established separately for each N. To display them clearly, Fig. 9 shows them according to the color of the output. After establishing N-step-ahead prediction models, for a specified input vector, N-step-ahead values are predicted according to the corresponding model. For example, in the testing time series, the first M data are selected as inputs for predicting the data for the subsequent N steps. First, the first-step-ahead data, namely, the M+1 data, are predicted based on the one-step-ahead model, whose outputs are both displayed in red. Then, the second-step-ahead data, namely, the M+2 data (green), are predicted according to the same input vector by the green model (the second-step-ahead prediction model). This procedure is repeated until at the last step N, the M + N data (purple) are predicted according to the purple model, which is the N-step-ahead prediction model. This is one complete case of M-N multi-step prediction. Via repeated prediction in the testing period, the uncertainty for each step can be quantified, as in the M-1 model.

3.3.3. M-1 slope model

Since the incoming weather conditions are closely related to the trend of the last several observations, the slope information between the last few data can be induced for prediction. The model in this study is called 'M-1 slope model'. The M-1 slope model is similar to the M-1 model, which is also based on a recursive process. However, there are several differences between these two models in the selection of training data. In the M-1 model, all data during the training period are included in the training dataset. In contrast, in the M-1 slope model, only data that have similar properties to the current data can be selected as training data. This means that for weather forecasting, to predict the future weather variations, it is necessary to find historical data that are similar to the current weather conditions and utilize them to predict the future weather. The selection criteria are the values and slopes of the current and previous data. The prediction procedure is as follows:

3.3.3.1. Selection of the training dataset. Assume the current time is t and denote the data by X(t). Find historical data X(t) during the training period that satisfy the following conditions:

a. |X(t)-X(t) | < an allowable error;
b. The symbols of the slopes at X(t) and X(t) are the same;
c. | slope at X(t) – slope at X(t) | < an allowable error;
d. The symbols of the slopes at X (t-1) and X(t-1) are the same;
e. | slope at X (t-1) – slope at X(t-1) | < an allowable error

Then, data X(t) can be selected. The corresponding input set (X(t-M+1), …, X(t-1), X(t)) and output X(t+1) can be selected as one training sample. After all the data that satisfy the above requirements have been selected, the prediction model can be established according to the corresponding training samples. In this method, allowable errors are determined based on the bivariate histogram of the parameter and its slope.

3.3.3.2. Prediction. After establishing the prediction model, (X(t-M+1), …, X(t-1), X(t)) is supplied to this model as input and one-step-ahead prediction $\widehat{X}(t+1)$ can be obtained.

3.3.3.3. Iteration. Next, the prediction $\widehat{X}(t+1)$ is utilized as the input and the input vector becomes (X(t-M+2), …, X(t), $\widehat{X}(t+1)$). Then, the training dataset is selected according to $\widehat{X}(t+1)$ and X(t). The selection process is the same as in 1). The prediction model based on the new training data is applied to obtain the two-step-ahead prediction $\widehat{X}(t+2)$. When no training data are available, the prediction process stops. Otherwise, the process is iterated until an N-step-ahead prediction, namely, $\widehat{X}(t+N)$, is obtained.

If all values from X(t+1) to X(t + N) must be predicted, N models must be constructed, similar to the M-N model. However, this model only applies historical data that have the same values and slopes as the current data to establish the prediction model, which could improve the prediction efficiency. In addition, compared with the M-1 model, the M-1 slope model may accumulate less error since the prediction model will be updated at each step ahead.

To illustrate the architecture of the M-1 slope model, the selection process of the training data in the M-1 slope model is sketched in Fig. 10. According to Fig. 10, a long-term time series of data is divided into training data and testing data. Instead of building a prediction model based on all training data, the first step is to select a suitable training data set in terms of the values and slopes of the testing data at points M and M-1. Here, the input vector consists of the first M data during testing period. Limited by the figure display, only the information of the point M is plotted in the figure. By taking advantage of this value and slope by adding an allowable error, a series of points within the yellow range can be identified in the training period (shown as red circles). The corresponding input-output pairs of these points can be selected as training data for predicting the next-step data. Then, using the value and slope of the predicted data X(M+1), another training data set can be identified for establishing a new prediction model and the second-step-ahead value

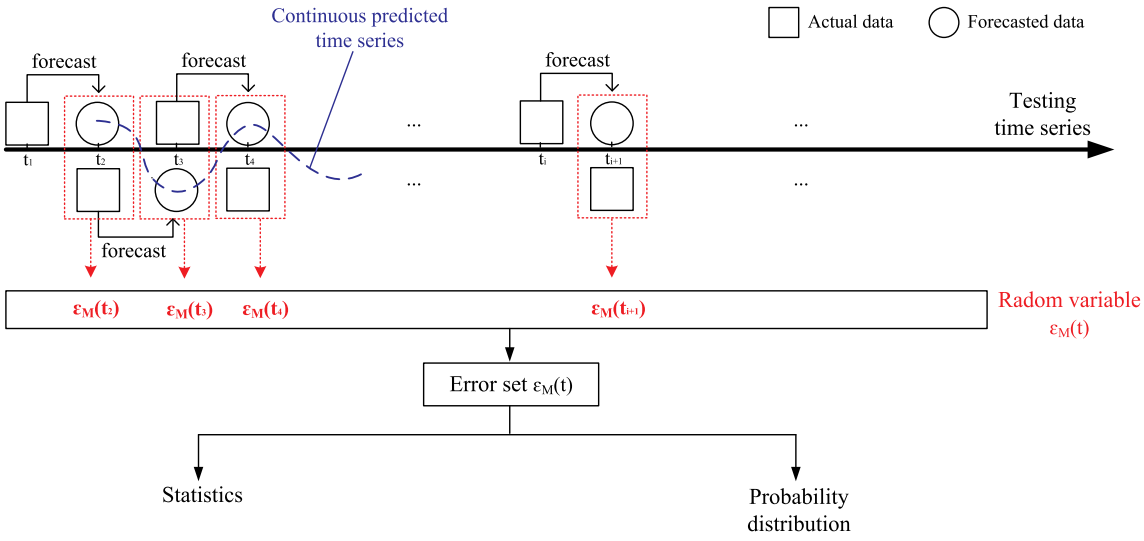

Fig. 11. Flowchart of uncertainty quantification analysis.

1. One-step-ahead prediction is performed by applying decomposition-ANIFS in the testing period. To obtain a continuous time series of predicted values, the selected input and corresponding output in the prediction model are illustrated in Fig. 11. In Fig. 11, square and circle marks represent the actual and forecasted data, respectively. For instance, actual data $a(t_1)$ is used to obtain predicted data $f(t_2)$; then, actual data $a(t_2)$ is used to obtain predicted data $f(t_3)$, and so on.
2. After prediction, forecast error factors are calculated via Eq. (20) using actual and forecasted data at the same time instant. For a testing time series, $\epsilon_M(t)$ is a random variable.
3. By statistically analyzing the realization of $\epsilon_M(t)$, its mean value and standard deviation can be calculated. In addition, a proper probability distribution of the forecast error factor can be fitted.

X(M+2) can be forecasted. Via this recursive process, the predicted time series (shown as the blue dashed line) can be obtained. To illustrate the process more clearly, a magnified image of the difference between the forecasted and the actual time series is plotted and the eight-step-ahead prediction procedure is also shown (the red circle within the purple range). After obtaining the forecasted time series, the same uncertainty quantification analysis can be conducted as described above.

In contrast to the previous two models, the M-1 slope model considers the slope of the data. Hence, the historical data cannot be considered when the slope is opposite that of the current data, even if the values are nearly the same. Via this approach, many irrelevant sea conditions can be removed, thereby significantly reducing the computation time compared to the M-N model. Furthermore, this method is essentially a recursive method that can preserve the complex dependencies among the forecasted data.

3.4. Uncertainty quantification

Traditionally, various error statistics have been used to measure the forecast accuracy, such as the mean absolute error (MAE), the root-mean-squared error (RMSE), and the mean absolute percentage error (MAPE). Most of these statistics are non-negative and the direction of the errors is not considered. However, in weather forecasting, the directions of forecast errors in various sea states are of great importance. Ignoring the directions of the errors would increase the risk of decision-making during the execution of marine operations. In addition, to account for the uncertainty in the forecasts, DNV (JIP, 2007) introduced a safety factor into the allowable limits of sea states that are used for marine operations. However, this alpha-factor approach has several limitations. For instance, the alpha-factor for significant wave height, depending on the prediction horizon is explicitly given in the DNV Offshore Standard, while this factor for other weather parameters (such as spectral peak period) has not been given yet. Meanwhile, the alpha-factor which is tabulated in the DNV Offshore Standard is only developed for the North and Norwegian Seas and is also dependent on the weather forecast techniques. In this section, an uncertainty quantification method is presented for improving the knowledge and understanding of a forecasting model for the short-term prediction of wind and wave conditions.

The accuracy of a forecasting model is evaluated by comparing the forecasts to corresponding actual values. To quantify environmental variables, the error must be normalized. For this purpose, a forecast error factor, which is denoted as $\epsilon_M(t)$, is introduced, which is utilized as an estimate of the forecast accuracy. This error factor is defined as the difference between the forecasted and actual values at the same time instant, normalized by the corresponding actual value:

$$\varepsilon_M(t) = \frac{f(t) - a(t)}{a(t)} \tag{20}$$

where $f(t)$ and $a(t)$ are the forecasted and actual values, respectively, at time t.

According to the above equation, a perfect weather forecast would yield a forecast error factor of 0. To assess the performance of a forecasting model under various sea states, all values of ϵ_M during the testing period must be calculated. Based on the series of ϵ_M values, the forecast uncertainty is quantified by the statistics (mean and standard deviation) and their distributions. For example, the methodology for estimating the uncertainty in a one-step-ahead prediction model is illustrated in Fig. 11. For multi-step-ahead forecasts, uncertainty quantification analysis is performed for each forecast time step. In addition, the quantified uncertainties can be utilized to provide a prediction range that is based on the multi-step-ahead predictions; the details are provided in Section 5.

3.5. Summary

This section describes the main procedures of the proposed method for predicting short-term weather conditions and assessing the forecasting performance. The whole prediction process is illustrated in Fig. 12 and the main steps are listed below.

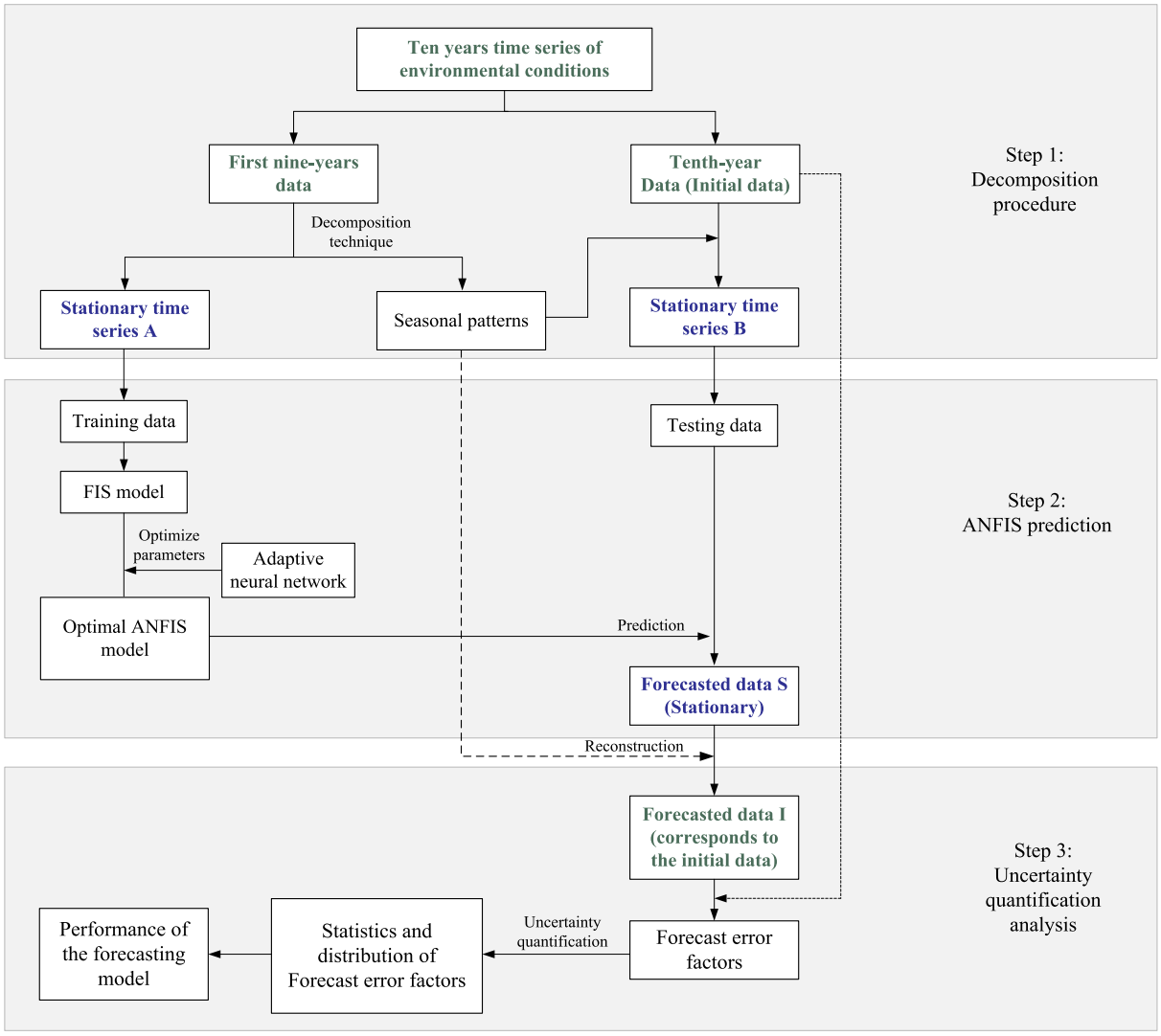

Fig. 12. Flowchart of the proposed method.

Step 1- Decomposition procedure: The objective of this step is to generate stationary time series. The long-term time series of environmental variables at a specified site is divided into two parts: The first part (most of the data) is called historical data (in this case study, it consists of the data of years 2001–2009) and can be decomposed into a stationary time series (referred to as stationary time series A here) and seasonal patterns (the monthly mean value vector and covariance matrix) via the decomposition technique that is described in Section 3.1. Meanwhile, the second part (a smaller portion of the data) is called study data (the data of year 2010 in this case study). This initial time series can be decomposed by using seasonal patterns that have been estimated from the first group to obtain the corresponding stationary time series (referred to as stationary time series B here). In this step, stationary times series for the first nine years and the tenth year can be determined for establishing and testing the prediction models in the next step.

Step 2- ANFIS prediction: In ANFIS prediction, the structure of the model depends on the number of prediction steps. If performing one-step-ahead prediction, the structure of the model can be established as in Eq. (13)-(15). For multi-step-ahead prediction, the model structure can correspond to the M-1, M-N or M-1 slope model. After determining the structure of the ANFIS, stationary time series A is selected as training data, which are utilized for the estimation of the optimal parameters of the model. This process is described in Section 3.2 in detail. Then, stationary time series B is referred to as the testing data, which are employed to evaluate the performance of the forecasting model. After prediction, the forecasted data S that correspond to stationary time series B can be obtained.

Step 3- Performance assessment: To assess the forecast performance of the prediction model, it is necessary to reconstruct the forecasted data I based on the forecasted data S along with seasonal patterns that were estimated from the first nine years. After that, the forecast error factor series can be calculated via Eq. (20) and the forecast uncertainty in the prediction model can be quantified using the statistics and distribution of this series.

4. Results and discussion

Referring to the execution time of the typical marine operation, the prediction period is expected to be more than one day; hence, N is selected as 24 in this study. Adopting the proposed prediction models, the '24 steps' case is conducted to predict U_w, H_s and T_p at the North Sea Center. Based on the results, a comparative analysis of the decomposition-ANFIS method with three multi-step-ahead forecasting models is performed. In the following parts, to demonstrate the forecasting performance of the decomposition-ANFIS method, the one-step-ahead prediction results are presented in Section 4.1 and the results of multi-step-ahead prediction are summarized in Section 4.2.

4.1. One-step-ahead prediction results

In this part, one-step-ahead models for predicting wave and wind conditions are developed. Three simple FIS models are represented by Eqs. (13)-(15), and the structure of the models are summarized in Table 1.

In each model, all input variables are partitioned into two fuzzy sets:

Table 1
Structures of the one-step-ahead FIS models.

No. of model	Output		Input			
	Variable	MF type	Variable	Fuzzy set	MF number	MF type
1	$Uw(t+1)$	linear	$Uw(t)$	'low','high'	2	Gaussian
2	$Hs(t+1)$	linear	$Uw(t)$	'low','high'	2	Gaussian
		linear	$Hs(t)$	'low','high'	2	Gaussian
3	$Tp(t+1)$	linear	$Uw(t)$	'low','high'	2	Gaussian
		linear	$H_s(t)$	'low','high'	2	Gaussian
		linear	$T_p(t)$	'low','high'	2	Gaussian

'Low' and 'High'. Gaussian-type MFs are selected for inputs and linear-type for the output. As a result, the total numbers of IF-THEN rules in the U_w, H_s and T_p prediction models are 2, 4 and 8, respectively. For instance, one of the rules of T_p prediction can be expressed as follows:

IF $U_w(t)$ is low, $H_s(t)$ is high, and $T_p(t)$ is high

THEN $T_p(t+1) = p_1 U_w(t) + q_1 H_s(t) + r_1 T_p(t)$

where p_1, q_1 and r_1 are the unknown parameters that must be determined from the training data.

After determining the structure of the FIS model, the training data are utilized to train this model and to optimize the parameters of FIS using neural networks. As an example, the MFs of H_s that are used in T_p prediction before and after training are plotted in Fig. 13. There are considerable changes in the shapes of the membership functions after training. It should be noted that the initial shape of MFs only depends on the type of MFs and the range of training data, which would enhance the reproducibility of this method.

After establishing the optimal ANFIS, testing data are used to evaluate the accuracy of the prediction method. The forecasted U_w, H_s and T_p and the corresponding actual data are plotted in Fig. 14(a), (b) and (c), respectively. In each subfigure, the blue lines are obtained using the actual data at the current time to predict the one-step-ahead environmental conditions. All the predicted data are presented in the figures and compared with the actual data.

According to Fig. 14, the forecasted data are close to the actual data in both wind and wave conditions throughout the entire testing period, which can also be observed in the distributions of the forecast error factors, as shown in Fig. 15. All three distributions of the forecast error factors of U_w, H_s and T_p predictions are concentrated around zero. In addition, the range of errors that are within one standard deviation of the mean (e.g., the range for U_w prediction, which is shown as red dash lines) is narrow; hence, the one-step-ahead prediction model has lower forecast uncertainty under various sea states. Therefore, the prediction method that combines the decomposition technique and ANFIS has high application potential for predicting environmental conditions. The detailed statistical results of the forecast error factor are included in the multi-step-ahead prediction results in Section 4.2.

4.2. Multi-step-ahead prediction results

4.2.1. Selection of the optimal model

In the multi-step-ahead forecasting models, the size of input set 'M' must be specified in advance. In practice, a suitable value for M is not easy to determine. Typically, if a larger amount of input data is available, more historical information can be utilized and, thus, predictions are expected to be more accurate. However, the computation time of a prediction model would increase dramatically with the number of inputs, especially if optimization techniques are required during the training phase. In this study, M is determined by comparing the forecast performances of multi-step-ahead prediction models under various values of M, starting from M = 1. The optimal value of M is the value that corresponds to the minimum statistics of forecast error factors for the predictions. In the M-1 model, the optimal value of M is selected by comparing the forecast uncertainties of all 24 steps because the computational burden is low. By contrast, in the M-N model, only the forecast uncertainties at a few steps are considered as criteria because this model demands a large computational effort compared to the M-1 model. In addition, the M-N model only uses actual data as inputs; hence, it is possible to apply many variables that are related to the predicted parameter for prediction. For example, historical wind conditions (such as wind speed and wind direction) can be applied to predict the future significant wave height. In addition, the structure of the M-N model may be more complicated and the corresponding computation time is longer. Therefore, the optimal M for the M-N model is selected by only comparing the forecast uncertainties at several specified steps.

4.2.1.1. M-1 model. In the following U_w, H_s and T_p predictions, M is varied from 1 to 5 to modify the structure of the prediction model. After establishing the model with a specified M, 24-step-ahead values are predicted iteratively. By repeatedly making 24-step-ahead predictions within the testing period, the statistical results of forecast error factors at each step N for various values of M are calculated and plotted in Fig. 16, where (a), (b) and (c) are the results of U_w, H_s and T_p, respectively. In each subfigure, the mean values and standard deviations of forecast error factors are represented by solid lines and dashed lines as functions of the number of steps N, individually. As illustrated in Fig. 16(a), the blue line, which corresponds to M = 2, is the optimal result since the mean values and the standard deviations for all steps are less than 0.2 and 0.8, respectively. In Fig. 16(b) and (c), M = 2 is a more suitable choice for H_s and T_p predictions in terms of both the forecast

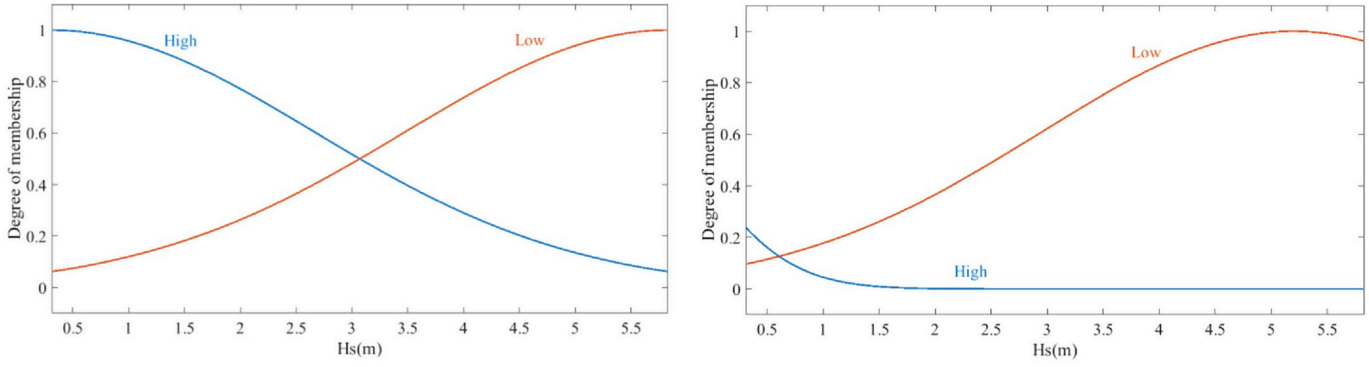

(a) before training (b) after training

Fig. 13. Shapes of membership functions.

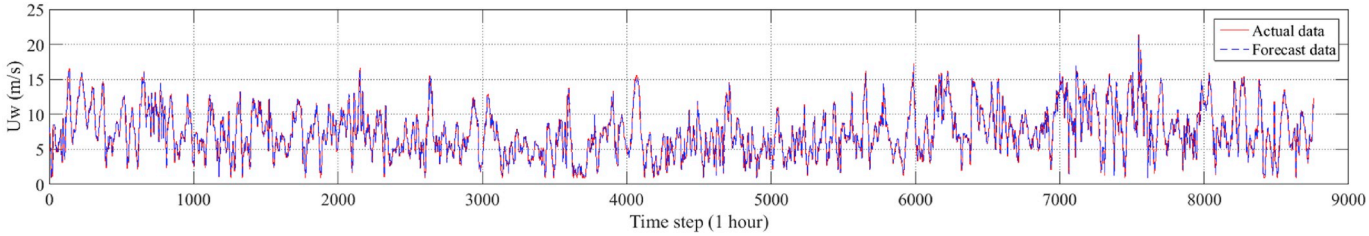

(a) U_w

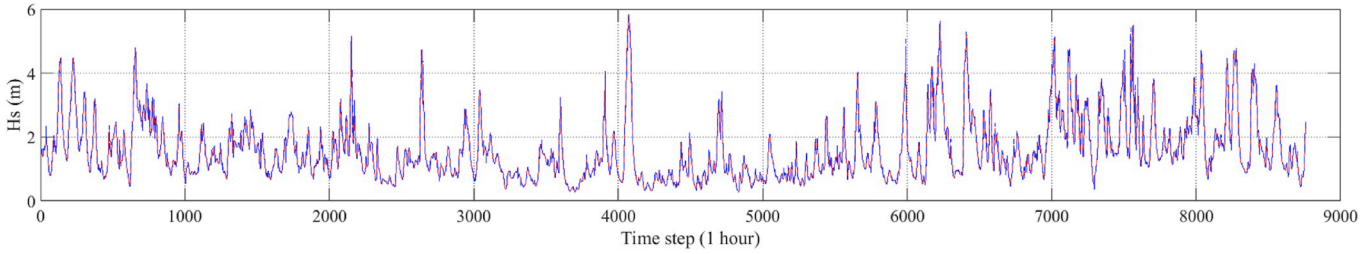

(b) H_s

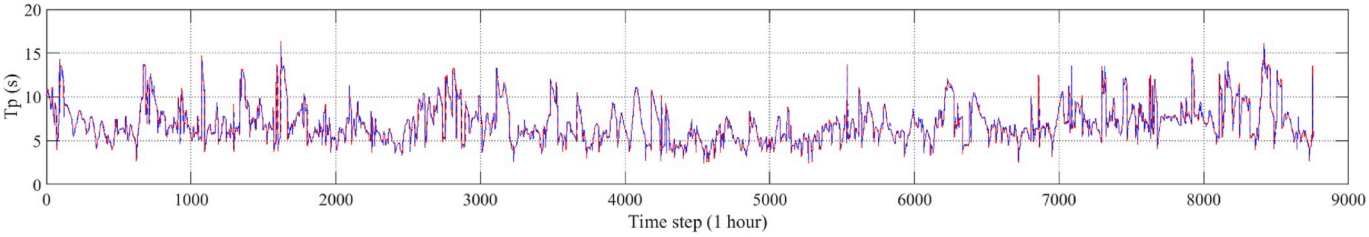

(c) T_p

Fig. 14. One-step-ahead prediction results.

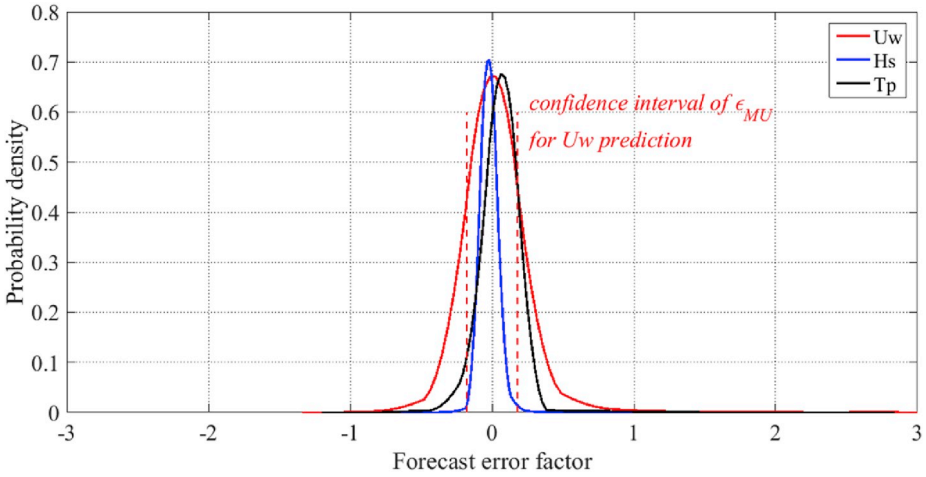

Fig. 15. Distributions of the forecast error factor (one-step-ahead prediction model).

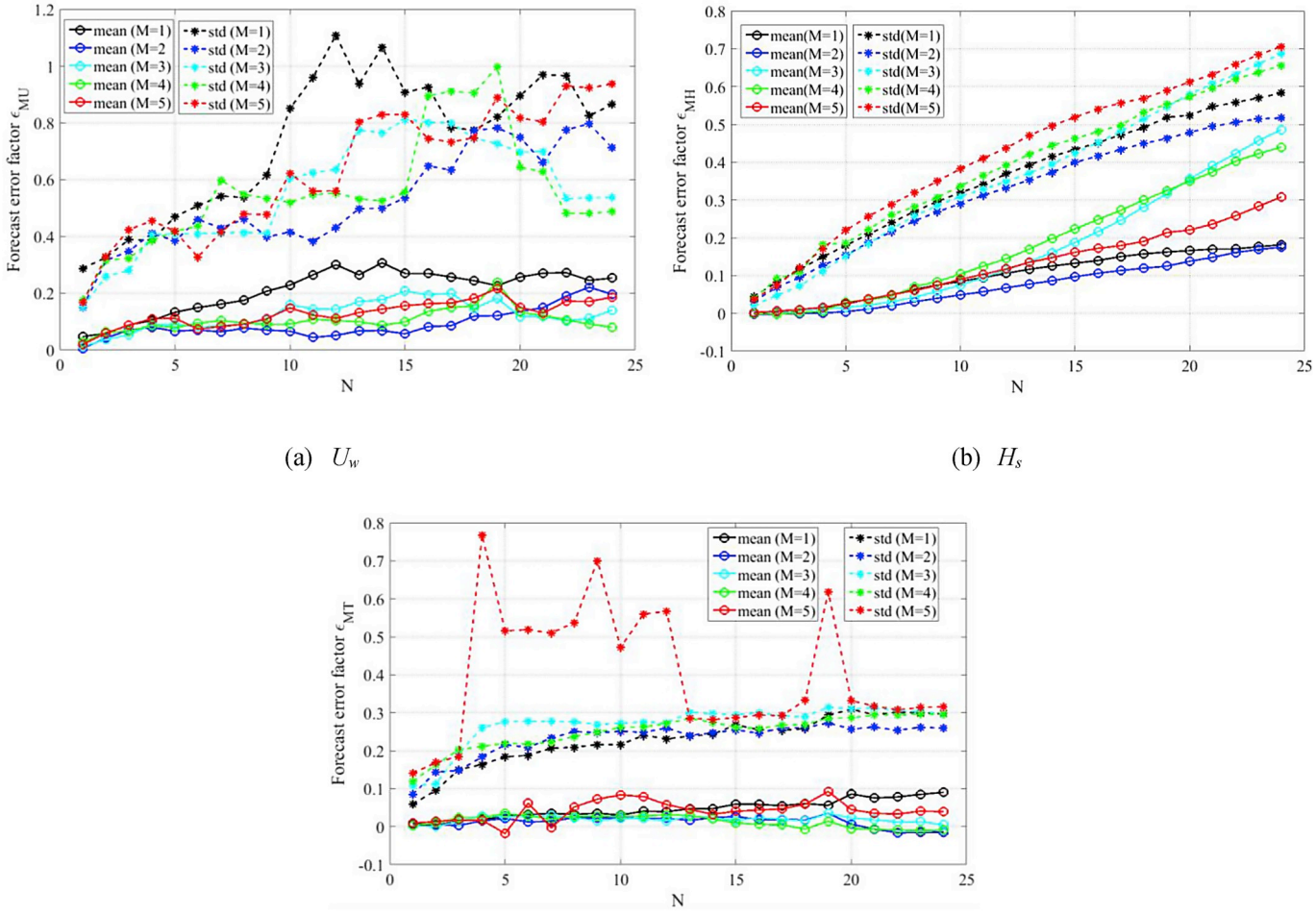

(a) U_w (b) H_s

(c) T_p

Fig. 16. Comparison of forecast uncertainties for various values of M (M-1 model).

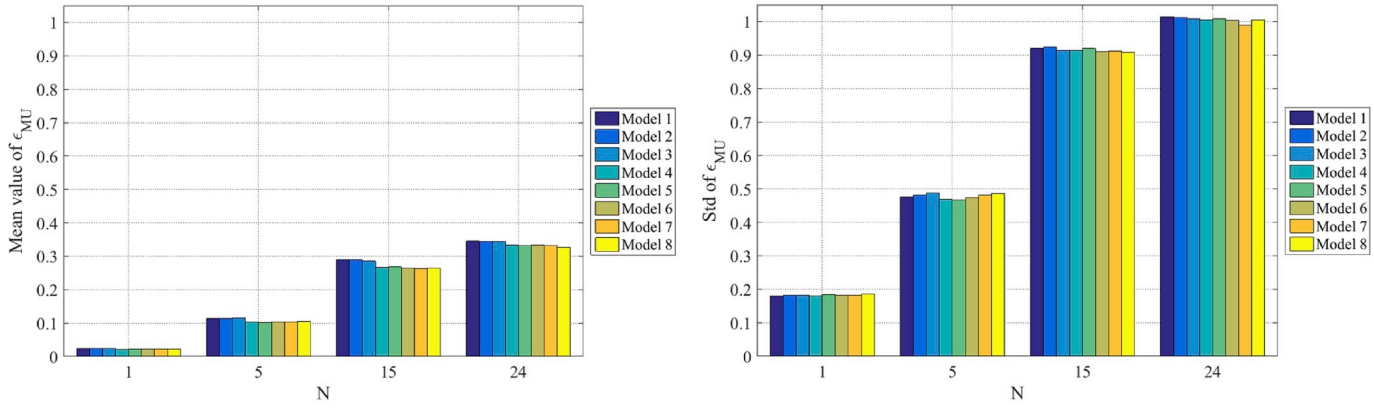

(a) Mean value (b) Standard deviation

Fig. 17. Forecast uncertainties in U_w prediction using various models.

performance and the computation time.

In summary, the optimal M-1 models for multi-step-ahead U_w, H_s and T_p predictions (with M = 2) are listed below Eqs. (22) and (23):

$$\mathrm{U}_w(\mathrm{t}+1) = f(\mathrm{U}_w(\mathrm{t}), \mathrm{U}_w(\mathrm{t}-3)) \tag{21}$$

$$\mathrm{H}_s(\mathrm{t}+1) = f(\mathrm{H}_s(\mathrm{t}), \mathrm{H}_s(\mathrm{t}-1)) \tag{22}$$

$$\mathrm{T}_p(\mathrm{t}+1) = f(\mathrm{T}_p(\mathrm{t}), \mathrm{T}_p(\mathrm{t}-1)) \tag{23}$$

In Eq. (21), the input terms are $U_w(t)$ and $U_w(t-3)$ instead of $U_w(t)$ and

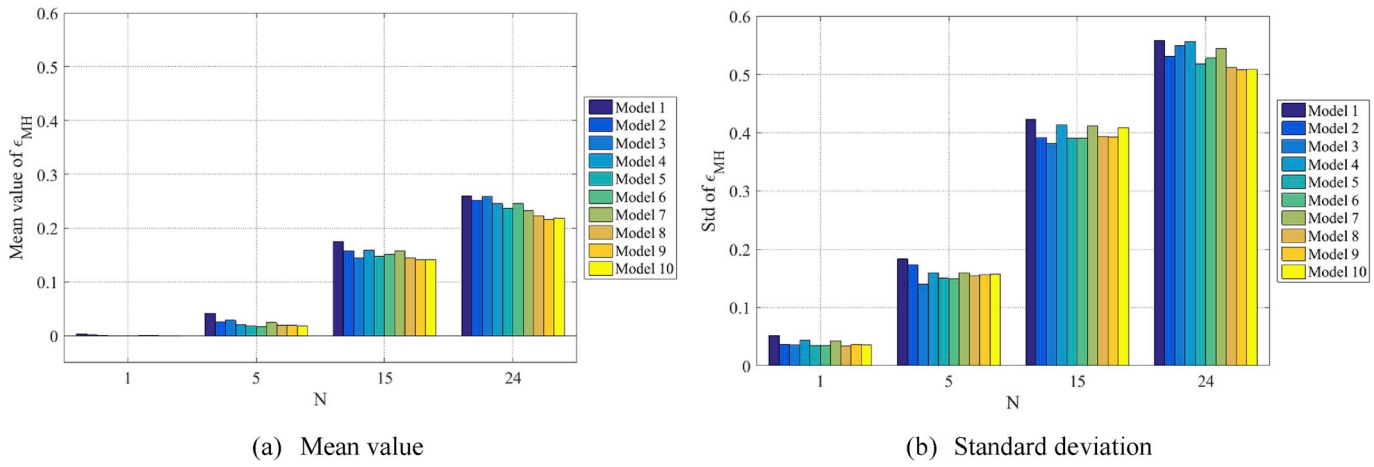

(a) Mean value (b) Standard deviation

Fig. 18. Forecast uncertainties in H_s prediction using various models.

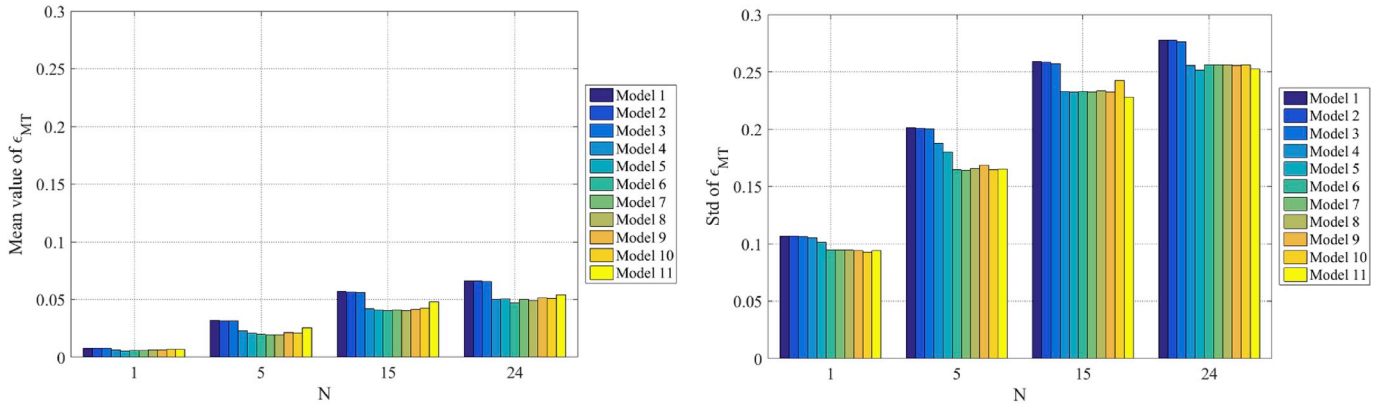

(a) Mean value (b) Standard deviation

Fig. 19. Forecast uncertainties in T_p prediction using various models.

$U_w(t\text{-}1)$ because the wind speed data are three-hourly data.

4.2.1.2. M-N model. To evaluate the influence of the value of M on the M-N model, prediction of the wind speed, the significant wave height and the peak spectral wave period will be discussed. In wind speed prediction, the historical data of wind direction (*Dir*) and wind speed (U_w) can be considered as input variables. The wind direction must be transformed to range between 0 and 1 (Sylaios et al., 2009), which is expressed as Eq. (24). U_w M-N models for various combinations of M and variables are listed in Table A.1 in the appendix. In the T_p and H_s M-N prediction models, as waves are influenced by the strength of the wind, models that consider wind variables such as the wind direction (*Dir*) and the wind speed (U_w) are also induced in an attempt to capture this dependency. The possible models of H_s and T_p are summarized in the appendix and described in Tables A.2 and A.3. Since the calculation time sharply increases with the size of the input set, only models with 6 or fewer items are considered.

$$Dir = \begin{cases} 1 - \left(\dfrac{\theta}{180}\right), & if\ 0^\circ \le \theta \le 180^\circ \\ \dfrac{(\theta - 180)}{180}, & if\ 180^\circ \le \theta \le 360^\circ \end{cases} \tag{24}$$

After determining the structure of the prediction models, several (1st, 5th, 15th and 24th) step-ahead predictions are made for each variable. After prediction, the statistics of forecast error factors for the corresponding models are summarized and plotted in Figs. 17–19.

As displayed in Fig. 17, there is not much difference in the prediction accuracy among models. However, the models (models 4–8) that include both U_w and *Dir* yield more accurate prediction results compared with the models (models 1–3) that are only based on U_w. A similar phenomenon can also be observed in Figs. 18 and 19. By considering both the computation time and the forecast uncertainty, the optimal U_w, H_s and T_p M-N prediction models are models 7, 9 and 6 in Tables A.1- A.3, respectively, which are listed below Eqs. 25, 26 and 27:

$$\mathrm{U}_w(\mathrm{t}+\mathrm{N}) = f(\mathrm{U}_w(\mathrm{t}),\ Dir(\mathrm{t}), \mathrm{U}_w(\mathrm{t}-3), \mathrm{U}_w(\mathrm{t}-6), \mathrm{U}_w(\mathrm{t}-9)) \tag{25}$$

$$\mathrm{H}_s(\mathrm{t}+\mathrm{N}) = f(\mathrm{H}_s(\mathrm{t}), \mathrm{U}_w(\mathrm{t}), Dir(\mathrm{t}), \mathrm{H}_s(\mathrm{t}-1), \mathrm{U}_w(\mathrm{t}-1)) \tag{26}$$

$$\mathrm{T}_p(\mathrm{t}+\mathrm{N}) = f\big(\mathrm{T}_p(\mathrm{t}), \mathrm{H}_s(\mathrm{t}), \mathrm{U}_w(\mathrm{t})\big) \tag{27}$$

The accuracy of the M-N model appears to be only slightly sensitive to the value of M. With the selected ANFIS configuration and data, there is no clear benefit in increasing M. However, due to heavy computational demand of running the ANFIS simulations, only relatively simple models with small M values are developed in this study. Since the use of more complex ANFIS models may improve the forecast accuracy, an effort can be considered to simulate ANFIS with more inputs in future researches. By contrast, the types of variables that are included in the prediction model have a strong impact on the accuracy for wind and waves. The more variables that are associated with the predicted value, the more accurate the obtained prediction. Thus, to decrease the forecast

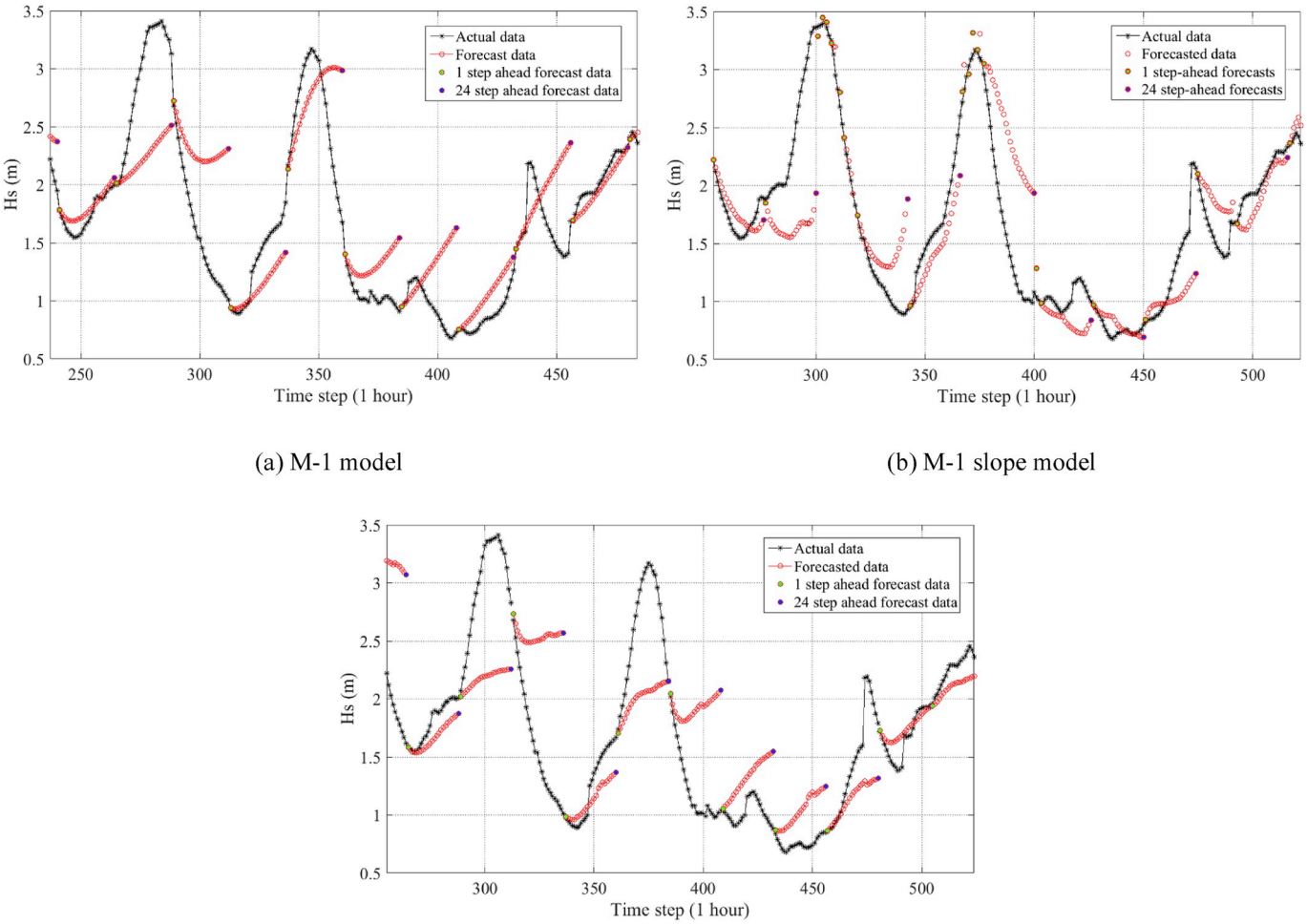

Fig. 20. Several cases of H_s prediction by the three models.

uncertainty in multi-step-ahead predictions, the variables that are related to the predicted parameter should be included if possible.

For the M-1 slope model, since it is essentially an iterative model, M is selected as 2 for all U_w, H_s and T_p prediction models by referring to the above sensitivity analysis results of the M-1 model.

4.2.2. *Comparison of the forecasting models*

This section presents a comparative analysis among the three multi-step-ahead forecasting models. At the beginning, three models of multi-step-ahead prediction, namely, the M-1, M-N and M-1 slope models, which use decomposition-ANFIS, are developed based on the training data. The input size M for each model is the optimal value that was determined in Section 4.2.1 and the forecast horizon is the following 24 h. Then, many twenty-four-step-ahead predictions can be obtained during the testing period on basis of the corresponding obtained prediction model. Finally, an uncertainty quantification analysis of the forecast error is conducted to assess the forecasting performances of the models.

The prediction results of U_w, H_s and T_p and the corresponding actual series are plotted in Fig. B.1, B.2 and B.3 in the appendix, in which the actual and forecasted data are represented by black and red lines. Subfigures (a) and (b) in each figure depict the results that are based on the M-1 and M-1 slope models and (c) depicts the results that are based on the M-N model. The predicted time series that were obtained iteratively and separately by applying the M-1 and M-N models consist of a few consecutive 24-step predictions, which correspond to the architectures in Figs. 8 and 9. By contrast, for the M-1 slope model, it may not be possible to predict 24 steps for all cases. To present the characteristics of the prediction models clearly, considering the H_s prediction as an example, several cases of prediction results that are based on the three models are extracted from Fig. B2 and shown in Fig. 20.

In each subfigure, the black lines depict actual time series and the predicted time series are represented by red lines. In addition, the green points correspond to the beginning of each 24-step prediction case, which correspond to one-step-ahead forecasted data. Similarly, the blue points represent the 24-step-ahead forecasted data. According to Fig. 20 (b), the M-1 slope model cannot perform the 24-step prediction in all cases, especially near the peaks of high sea states. However, compared to the results in Fig. 20(a) and (c), the M-1 slope model can capture the data variation, although the positions of peaks/troughs may not be captured exactly.

Overall, from the predicted time series in Fig. B1-B.3, it is concluded that the proposed models can predict the environmental conditions to a certain extent. However, due to the randomness in the occurrence of waves and wind, it is difficult to realize high accuracy in forecasting all points, especially for high sea states. In addition, only observing the long-term forecasted time series renders it difficult to compare the proposed three prediction models. Therefore, the uncertainty quantification analysis must be used to evaluate and compare the accuracies of the three multi-step-ahead prediction methods.

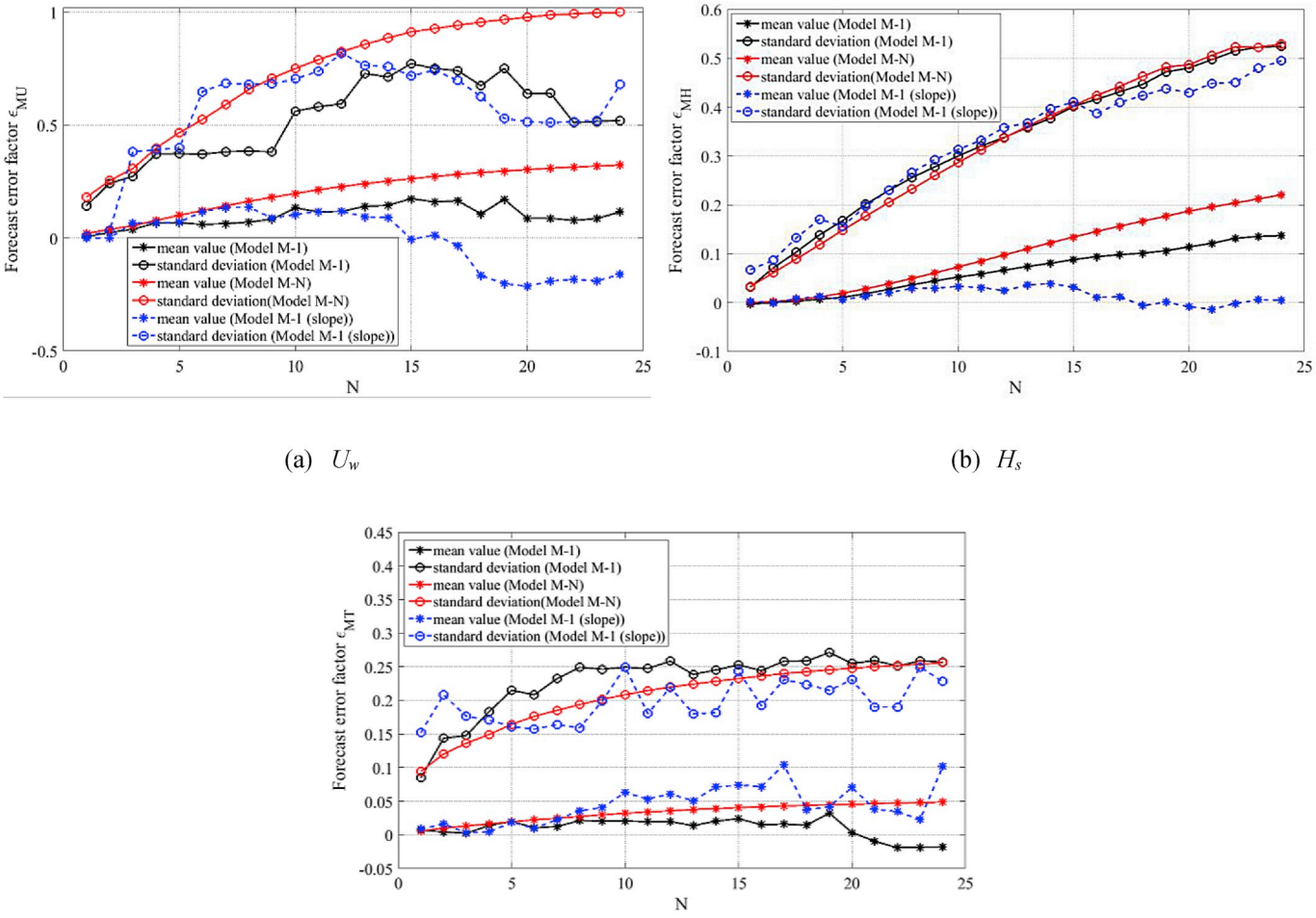

Fig. 21. Statistics of ϵ_M for N steps ahead.

Fig. 21 presents the results of multi-step-ahead forecasting models in predicting U_w, H_s and T_p at various steps N. In each subfigure, black, red and blue lines represent statistics of the corresponding forecast error factors ϵ_M that are based on the M-1 model, the M-N model and the M-1 slope model, respectively. To distinguish the statistics, the mean values are represented by circle marks and the asterisks correspond to the standard deviations.

The forecast uncertainty varies with the step N in both wind and wave condition predictions. The forecast error of the M-N model exhibits monotonic behavior with respect to the prediction step, whereas the forecast errors of the other two models exhibit variations because predicted values are used in the other two models. Fig. 21(a) compares the models in terms of forecast performance for the wind speed U_w. Among the three proposed multi-step-ahead forecasting models, the M-1 and M-1 slope models outperform the M-N model. As N increases, the forecast uncertainty of the M-N model significantly increases, which is reflected in the mean value and the standard deviation of the 24th step, which reach 0.33 and 1, respectively. This increase in uncertainty may be because the wind speed time series is so random that there is little correlation between the current data and the data for the following few hours. In the comparative analysis of the M-1 and M-1 slope models, when N is large, the mean values of the forecast error factors are positive and negative, respectively. As a result, the M-1 model can be considered the best performing model for U_w prediction since its prediction is relatively conservative.

Fig. 21(b) shows the H_s prediction. All three models yield almost identical results at the first step. At this step, the forecast uncertainties from the three models are low, as reflected in the near-zero mean values and standard deviations. With the increase of the forecast horizon, the M-1 slope model shows lower forecast uncertainty compared with the other two methods. By inspecting Fig. 21(b), although the standard deviation of the forecast error factors from the three models are similar, the mean values of the errors from the M-1 slope model are lower. For example, for N = 24, the mean values of the forecast error factors that are obtained using the M-1 model and the M-N model are 0.14 and 0.22, respectively, compared to only 0.004 for the M-1 slope model; hence, the M-1 slope model outperforms the others.

In Fig. 21(c), the T_p forecast performances for the three multi-step-ahead prediction models are displayed. The level of uncertainty is lower than in H_s and U_w predictions. All three models yield satisfactory results since the mean values and standard deviations of the forecast error factor for all steps are less than 0.1 and 0.28, respectively. Comparing the statistical results, the M-N method can provide more stable multi-step-ahead predictions at any step. This can be observed in the lower fluctuation of the forecast performance as functions of the forecast lead time. Thus, the M-N model performs the best in predicting multi-step T_p.

According to Fig. 21, as the lead time increases, the forecast uncertainty increases for all multi-step-ahead forecasting methods. To display it clearly, a probability distribution of the forecast error factor is used to describe forecast uncertainty at each step. For example, Fig. 22 shows forecast error distributions in T_p prediction for various values of N. In

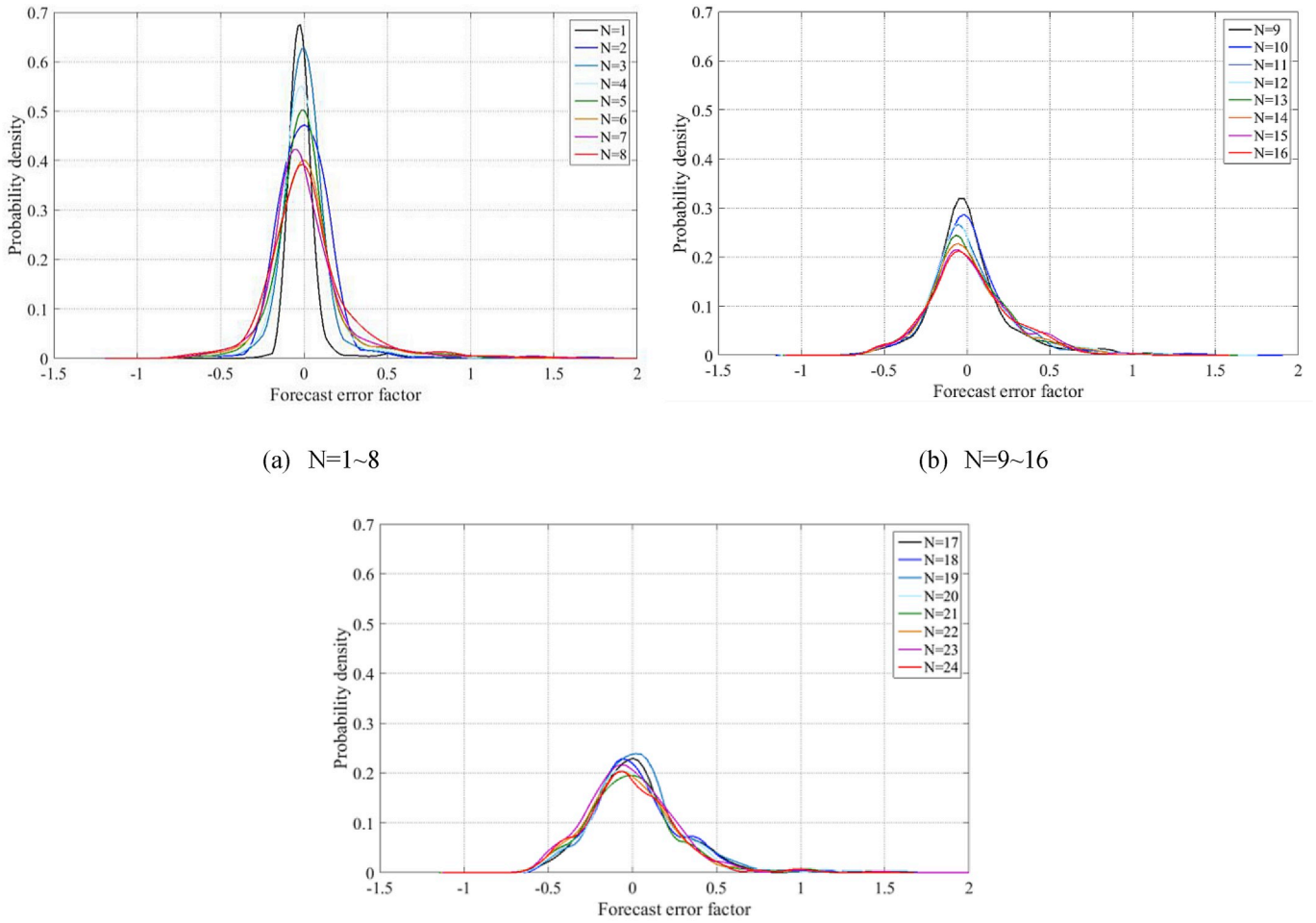

Fig. 22. Distributions of ϵ_{MT} (M-N model).

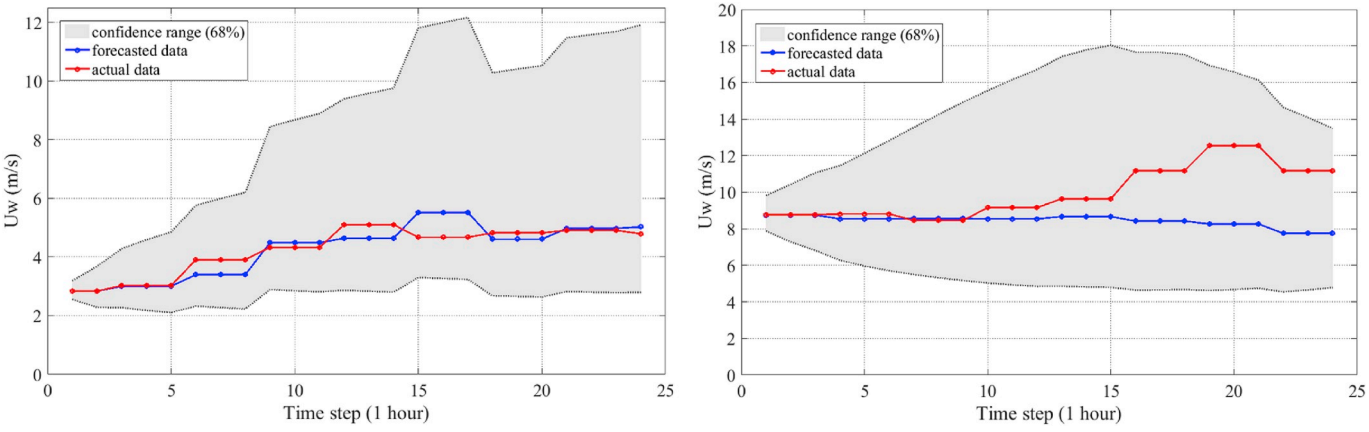

Fig. 23. U_w prediction ranges.

Fig. 22a), the distributions are more concentrated around the mean value in the cases with small N; hence, there is a lower forecast uncertainty for lead times from 1 to 8 h ahead. However, as N increases, the distributions become increasingly wide; hence, the uncertainty in the forecasts increases. Most of the forecast errors prior to the 8th step are concentrated between −0.3 and 0.3, while those after the 8th step are in the range of −0.6 to 0.6.

As illustrated above, the forecast horizon has an important effect on the performances of the multi-step-ahead forecasting models in predicting both wind and wave conditions. By applying the combination of the decomposition technique and ANFIS, the environmental conditions one to five steps ahead can be predicted accurately. However, due to the error accumulation problem of the M-1 and M-1 slope models and the uncorrelated input-output sample in the M-N model, the performances

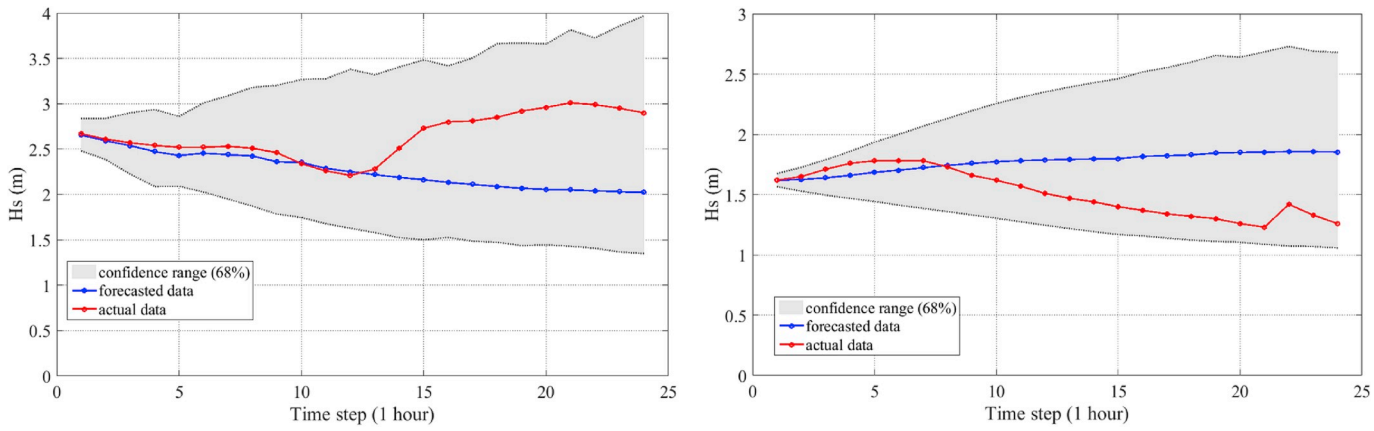

Fig. 24. H_s prediction ranges.

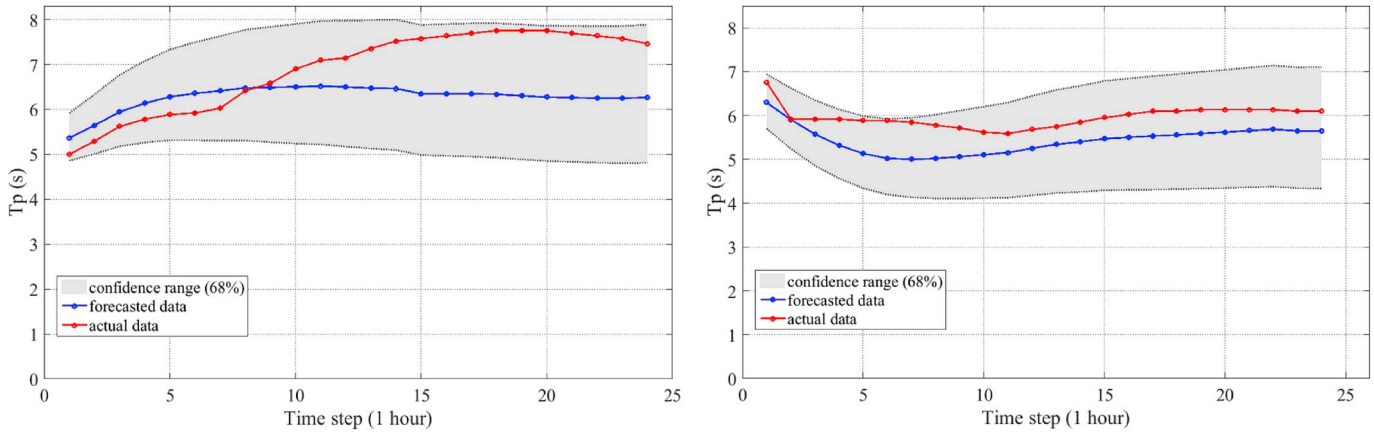

Fig. 25. T_p prediction ranges.

of all three multi-step-ahead prediction models deteriorate as N increases.

Under the circumstances, for a specified-step prediction, the mean value and the standard deviation of the errors can be utilized to provide a prediction range, instead of a single forecasted point. Based on the central limit theorem, the distribution of the forecast error factor can be approximated by a normal distribution. According to the properties of the normal distribution, 68% of the error is contained within one standard deviation of the mean, namely, within [m-σ, m+σ]. Applying this error range to the predicted value $f(t)$, a prediction range $R_a(t)$ is calculated via Eq. (20). This range can be expressed as Eq. (28), where it is expected to cover the future actual weather conditions.

$$R_{a(t)} = \frac{f(t)}{1 + m \pm std} \tag{28}$$

where m and std are the mean value and the standard deviation of the forecast error factor and $f(t)$ is the forecasted data at time t.

Through the above process, the future data at a specified step ahead can be represented by a range $R_{a(t)}$ rather than a separate prediction point $f(t)$. Via this approach, the high-uncertainty prediction can be used in practice. To evaluate the proposed method, two typical examples are selected for each environmental parameter and the prediction ranges for the following 24 h are identified from the fitted error curves. The corresponding prediction ranges of U_w, H_s and T_p are shown in Figs. 23–25, respectively. Each subfigure depicts one example, including the predicted and actual data and the prediction range.

According to all three figures, although the red and blue lines differ, which demonstrates that the forecasts may not be accurate for all 24 steps ahead, the prediction ranges (grey areas) always contain the actual data. Hence, if the accuracy of a large-step-ahead prediction is too uncertain to be adopted, the prediction range can provide guidance for the variation of the future sea state. Therefore, it is concluded that the proposed method is effective in capturing the future weather conditions in practice.

In addition, in Fig. 23(b), as the number of prediction steps increases, the prediction range does not always widen because the M-1 model uses forecasted data for prediction, which will lead to error accumulation. This situation is not realistic, especially if the number of forecast steps is further increased. As a result, the M-N model may be considered the most appropriate model for applying the prediction range for a long forecast horizon.

5. Conclusions

Predicting short-term wind and wave conditions is an important part of decision-making during the execution of marine operations. This work proposes a hybrid multi-step-ahead prediction model for predicting wind and wave conditions and investigates the forecast uncertainties in the suggested model over various seasons and sea states.

A hybrid method that combines a decomposition technique and ANFIS is introduced. In this method, the decomposition technique is applied to convert the original series to the corresponding stationary series to improve the overall forecasting accuracy. Then, the ANFIS is established, in which the input-output pairs are determined by three multi-step-ahead models: the M-1, M-N and M-1 slope models. Finally, by utilizing the three multi-step-ahead forecasting models, twenty-four-step-ahead predictions can be obtained recursively or directly. To

evaluate the efficiency of the proposed method, hourly time series of the mean wind speed (U_w), the significant wave height (H_s) and the peak spectral wave period (T_p) at the North Sea center are utilized. The results demonstrate that the proposed decomposition-ANFIS method performs well in one-step-ahead wave and wind forecasting. By contrast, the multi-step-ahead prediction models are more complex and the forecast accuracy decreases as the forecast horizon increases.

To quantify the forecast performance of the proposed method and to compare it with various multi-step-ahead models, an uncertainty quantification analysis is proposed. In the analysis, the forecast uncertainty for each model is assessed in terms of the forecast error factor. For a specified multi-step-ahead prediction model, by statistically analyzing a set of the forecast error factors that were obtained during the testing period, the forecast performance at each forecast step can be evaluated. Based on the quantification results, the optimal values of M of three multi-step-ahead models can be determined. In addition, three optimal multi-step-ahead models are also compared on both wind and wave predictions. The results demonstrate that the prediction model performance strongly depends on the properties of the variable. For U_w, H_s and T_p predictions, the best performing model is M-1, followed by M-1 slope and M-N. Typically, the proposed methods can effectively obtain exact predictions for the first five steps ahead due to the lower level of uncertainty. However, the uncertainty of forecasts will increase with the forecast horizon. Fitted equations of the mean and standard deviation of the forecast errors can be utilized to provide a prediction range instead of prediction points. Case studies demonstrate that this is an effective approach for utilizing the multi-step-ahead predictions in practice.

Overall, the proposed decomposition-ANFIS multi-step-ahead forecasting methods can be applied for the short-term prediction of wave and wind conditions and have application potential in marine operations. However, the randomness and unsteadiness of wind and waves render forecasting highly difficult for longer forecast horizons. The forecast uncertainty quantification method can overcome this problem; however, additional efforts to improve the accuracy of the proposed hybrid prediction models are necessary.

Acknowledgement

This work was supported by the Centre for Ships and Ocean Structures (CeSOS) and Centre for Autonomous Marine Operations and Systems (AMOS), at the Department of Marine Technology, NTNU, Trondheim, Norway. The support is gratefully acknowledged by the authors.

Appendix A. List of possible M-N models

Table A.1
U_w M-N prediction models

No. of model	Considered variables	M	Number of items	Model
1	U_w	2	2	$U_w(t+N) = f(U_w(t), U_w(t-3))$
2	U_w	3	3	$U_w(t+N) = f(U_w(t), U_w(t-3), U_w(t-6))$
3	U_w	4	4	$U_w(t+N) = f(U_w(t), U_w(t-3), U_w(t-6), U_w(t-9))$
4	U_w, *Dir*	2	3	$U_w(t+N) = f(U_w(t), Dir(t), U_w(t-3))$
5	U_w, *Dir*	2	4	$U_w(t+N) = f(U_w(t), Dir(t), U_w(t-3), Dir(t-3))$
6	U_w, *Dir*	3	4	$U_w(t+N) = f(U_w(t), Dir(t), U_w(t-3), U_w(t-6))$
7	U_w, *Dir*	4	5	$U_w(t+N) = f(U_w(t), Dir(t), U_w(t-3), U_w(t-6), U_w(t-9))$
8	U_w, *Dir*	5	6	$U_w(t+N) = f(U_w(t), Dir(t), U_w(t-3), U_w(t-6), U_w(t-9), U_w(t-12))$

Table A.2
H_s M-N prediction models

No. of model	Considered variables	M	Number of items	Model
1	H_s	1	1	$H_s(t+N) = f(H_s(t))$
2	H_s	2	2	$H_s(t+N) = f(H_s(t), H_s(t-1))$
3	H_s	3	3	$H_s(t+N) = f(H_s(t), H_s(t-1), H_s(t-2))$
4	H_s, U_w	1	2	$H_s(t+N) = f(H_s(t), U_w(t))$
5	H_s, U_w	2	4	$H_s(t+N) = f(H_s(t), U_w(t), H_s(t-1), U_w(t-1))$
6	H_s, U_w	2	3	$H_s(t+N) = f(H_s(t), U_w(t), H_s(t-1))$
7	H_s, U_w	1	3	$H_s(t+N) = f(H_s(t), U_w(t), Dir(t))$
8	H_s, U_w, *Dir*	2	4	$H_s(t+N) = f(H_s(t), U_w(t), Dir(t), H_s(t-1))$
9	H_s, U_w, *Dir*	2	5	$H_s(t+N) = f(H_s(t), U_w(t), Dir(t), H_s(t-1), U_w(t-1))$
10	H_s, U_w, *Dir*	2	6	$H_s(t+N) = f(H_s(t), U_w(t), Dir(t), H_s(t-1), U_w(t-1), Dir(t-1))$

Table A.3
T_p M-N prediction models

No. of model	Considered variables	M	Number of items	Model
1	T_p	1	1	$T_p(t+N) = f(T_p(t))$
2	T_p	2	2	$T_p(t+N) = f(T_p(t), T_p(t-1))$
3	T_p	3	3	$T_p(t+N) = f(T_p(t), T_p(t-1), T_p(t-2))$
4	T_p, H_s	1	2	$T_p(t+N) = f(T_p(t), H_s(t))$
5	T_p, H_s	2	4	$T_p(t+N) = f(T_p(t), H_s(t), T_p(t-1), H_s(t-1))$
6	T_p, H_s, U_w	1	3	$T_p(t+N) = f(T_p(t), H_s(t), U_w(t))$
7	T_p, H_s, U_w	2	4	$T_p(t+N) = f(T_p(t), H_s(t), U_w(t), T_p(t-1))$
8	T_p, H_s, U_w	3	5	$T_p(t+N) = f(T_p(t), H_s(t), U_w(t), T_p(t-1), T_p(t-2))$

(*continued on next page*)

Table A.3 (*continued*)

No. of model	Considered variables	M	Number of items	Model
9	T_p, H_s, U_w	2	5	$T_p(t+N) = f(T_p(t), H_s(t), U_w(t),\ T_p(t-1),\ H_s(t-1))$
10	T_p, H_s, U_w	2	6	$T_p(t+N) = f(T_p(t), H_s(t), U_w(t),\ T_p(t-1),\ H_s(t-1),\ U_w(t-1))$
11	T_p, H_s, U_w, *Dir*	1	4	$T_p(t+N) = f(T_p(t), H_s(t), U_w(t), \mathit{Dir}(t))$

Appendix B. Forecasted and actual time series in the testing phase

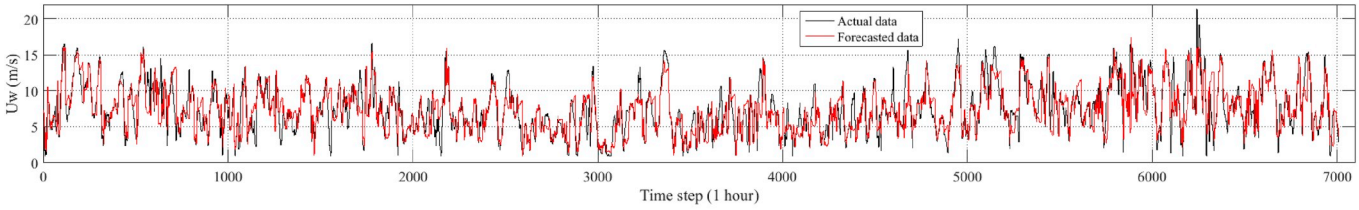

(a) M-1 model

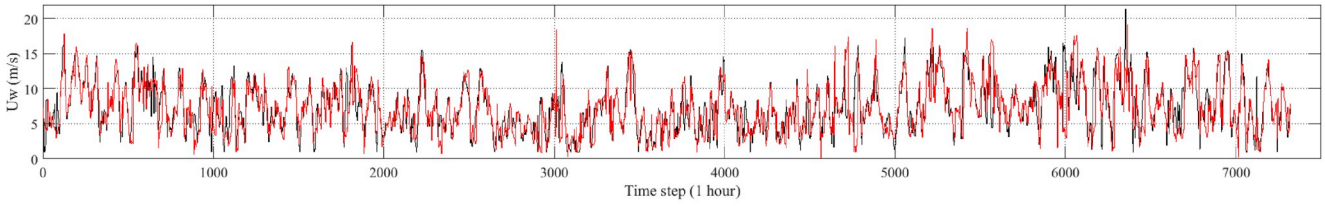

(b) M-1 slope model

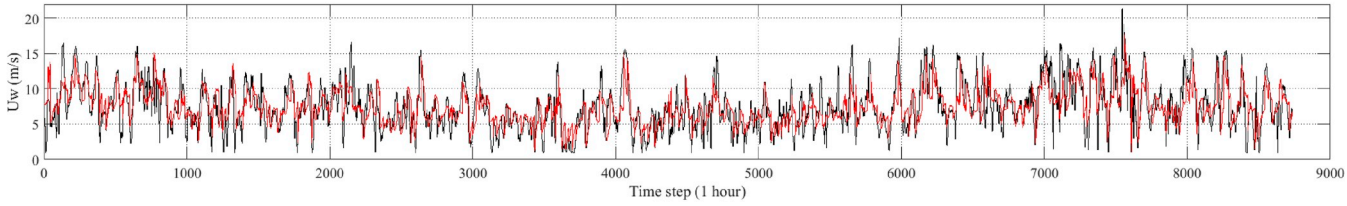

(c) M-N model

Figure B.1. Predicted time series of U_w.

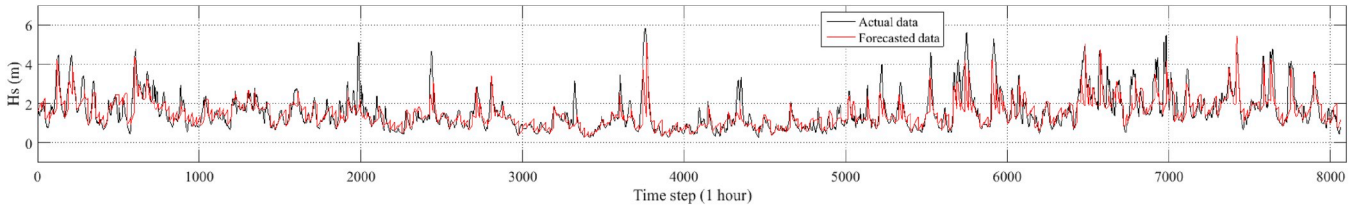

(a) M-1 model

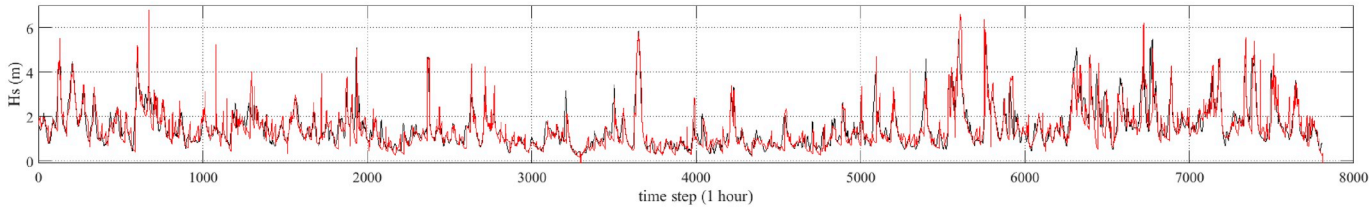

(b) M-1 slope model

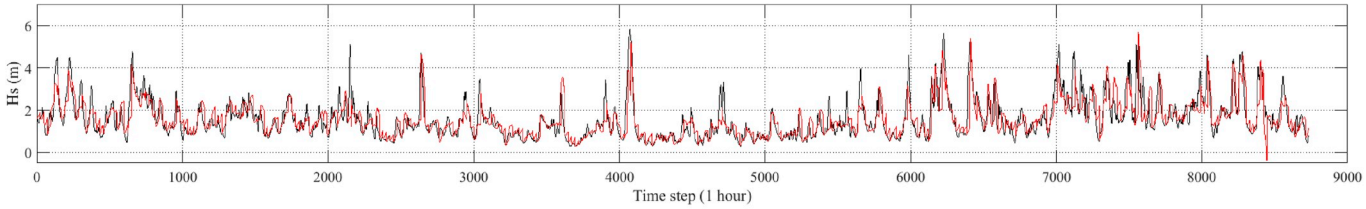

(c) M-N model

Figure B.2. Predicted time series of H_s.2

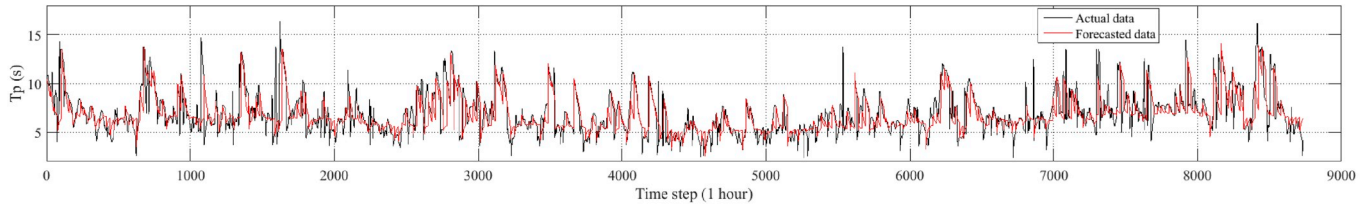

(a) M-1 model

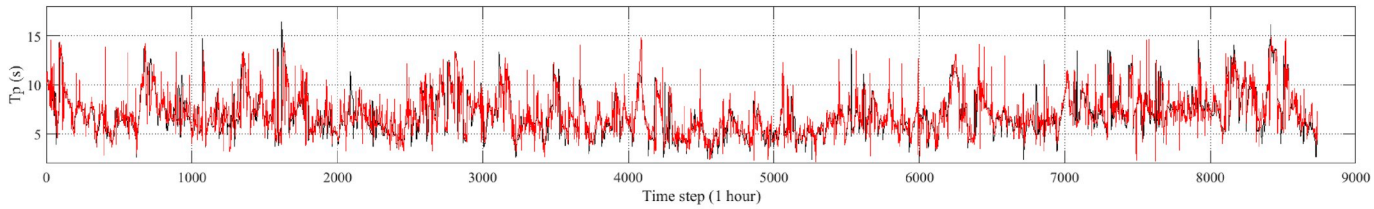

(b) M-1 slope model

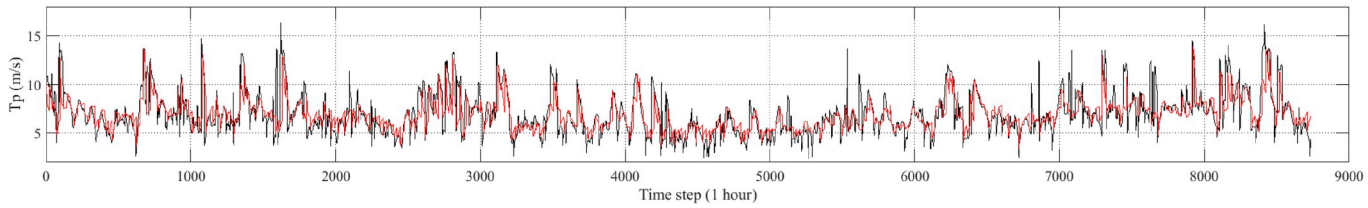

(c) M-N model

Figure B.3. Predicted time series of T_p.3

Appendix C. Supplementary data

Supplementary data to this article can be found online at https://doi.org/10.1016/j.oceaneng.2019.106300.

References

Acero, W.G., Li, L., Gao, Z., Moan, T., 2016. Methodology for assessment of the operational limits and operability of marine operations. Ocean. Eng. 125, 308–327.

Agrawal, J., Deo, M., 2002. On-line wave prediction. Mar. Struct. 15 (1), 57–74.

Ahmed, A., Khalid, M., 2017. Multi-step ahead wind forecasting using nonlinear autoregressive neural networks. Energy Procedia 134, 192–204.

Akpınar, A., Özger, M., Kömürcü, M.I., 2014. Prediction of wave parameters by using fuzzy inference system and the parametric models along the south coasts of the Black Sea. J. Mar. Sci. Technol. 19 (1), 1–14.

Al-Yahyai, S., Charabi, Y., Gastli, A., 2010. Review of the use of numerical weather prediction (NWP) models for wind energy assessment. Renew. Sustain. Energy Rev. 14 (9), 3192–3198.

Athanassoulis, G., Stefanakos, C.N., 1995. A nonstationary stochastic model for long-term time series of significant wave height. J. Geophys. Res.: Oceans 100 (C8), 16149–16162.

Basu, S., Sarkar, A., Satheesan, K., Kishtawal, C., 2005. Predicting wave heights in the north Indian Ocean using genetic algorithm. Geophys. Res. Lett. 32 (17).

Berbić, J., Ocvirk, E., Carević, D., Lončar, G., 2017. Application of neural networks and support vector machine for significant wave height prediction. Oceanologia 59 (3), 331–349.

Bishop, C.T., 1983. Comparison of manual wave prediction models. J. Waterw. Port, Coast. Ocean Eng. 109 (1), 1–17.

Booij, N., Ris, R.C., Holthuijsen, L.H., 1999. A third-generation wave model for coastal regions: 1. Model description and validation. J. Geophys. Res.: Oceans 104 (C4), 7649–7666.

Bretschneider, C.L., 1970. Forecasting relations for wave generation. Look Lab/Hawaii 1 (3), 31–34.

Browne, M., Castelle, B., Strauss, D., Tomlinson, R., Blumenstein, M., Lane, C., 2007. Near-shore swell estimation from a global wind-wave model: spectral process, linear, and artificial neural network models. Coast Eng. 54 (5), 445–460.

Cassola, F., Burlando, M., 2012. Wind speed and wind energy forecast through Kalman filtering of Numerical Weather Prediction model output. Appl. Energy 99, 154–166.

Chang, G., Lu, H., Chang, Y., Lee, Y., 2017. An improved neural network-based approach for short-term wind speed and power forecast. Renew. Energy 105, 301–311.

Deo, M., Naidu, C.S., 1998. Real time wave forecasting using neural networks. Ocean. Eng. 26 (3), 191–203.

Deo, M.C., Jha, A., Chaphekar, A., Ravikant, K., 2001. Neural networks for wave forecasting. Ocean. Eng. 28 (7), 889–898.

Donelan, M.A., 1980. Similarity Theory Applied to the Forecasting of Wave Heights, Periods and Directions. National Water Research Institute.

Duru, O., Yoshida, S., 2012. Modeling principles in fuzzy time series forecasting. In: 2012 IEEE Conference on Computational Intelligence for Financial Engineering & Economics (CIFEr). IEEE, pp. 1–7.

Erdem, E., Shi, J., 2011. ARMA based approaches for forecasting the tuple of wind speed and direction. Appl. Energy 88 (4), 1405–1414.

Foley, A.M., Leahy, P.G., Marvuglia, A., McKeogh, E.J., 2012. Current methods and advances in forecasting of wind power generation. Renew. Energy 37 (1), 1–8.

Group, T.W., 1988. The WAM model—a third generation ocean wave prediction model. J. Phys. Oceanogr. 18 (12), 1775–1810.

Hasselmann, K., Barnett, T., Bouws, E., Carlson, H., Cartwright, D., Enke, K., Ewing, J., Gienapp, H., Hasselmann, D., Kruseman, P., 1973. Measurements of wind-wave growth and swell decay during the joint North Sea wave project (JONSWAP). Ergänzungsheft 8–12.

Jain, P., Deo, M., 2007. Real-time wave forecasts off the western Indian coast. Appl. Ocean Res. 29 (1–2), 72–79.

Jang, J.-S., 1993. ANFIS: adaptive-network-based fuzzy inference system. IEEE Trans. Syst. Man Cybern. 23 (3), 665–685.
Jang, J.S.R., Sun, C.T., Mizutani, E., 1996. Neuro-fuzzy and Soft Computing; a Computational Approach to Learning and Machine Intelligence.
Jiang, Z., Gao, Z., Ren, Z., Li, Y., Duan, L., 2018. A parametric study on the final blade installation process for monopile wind turbines under rough environmental conditions. Eng. Struct. 172, 1042–1056.
JIP, D., 2007. Technical Report, Marine Operation Rules, Revised Alpha Factor—Joint Industry Project. DNV, Oslo.
Kamal, L., Jafri, Y.Z., 1997. Time series models to simulate and forecast hourly averaged wind speed in Quetta, Pakistan. Sol. Energy 61 (1), 23–32.
Kamranzad, B., Etemad-Shahidi, A., Kazeminezhad, M., 2011. Wave height forecasting in Dayyer, the Persian Gulf. Ocean. Eng. 38 (1), 248–255.
Kavasseri, R.G., Seetharaman, K., 2009. Day-ahead wind speed forecasting using f-ARIMA models. Renew. Energy 34 (5), 1388–1393.
Kazeminezhad, M., Etemad-Shahidi, A., Mousavi, S., 2005. Application of fuzzy inference system in the prediction of wave parameters. Ocean. Eng. 32 (14–15), 1709–1725.
Kazeminezhad, M., Etemad-Shahidi, A., Mousavi, S., 2007. Evaluation of neuro fuzzy and numerical wave prediction models in Lake Ontario. J. Coast. Res. 317–321.
Landberg, L., 1999. Short-term prediction of the power production from wind farms. J. Wind Eng. Ind. Aerodyn. 80 (1–2), 207–220.
Landberg, L., Myllerup, L., Rathmann, O., Petersen, E.L., Jørgensen, B.H., Badger, J., Mortensen, N.G., 2003. Wind resource estimation—an overview. Wind Energy 6 (3), 261–271.
Li, L., Gao, Z., Moan, T., 2013. Joint environmental data at five european offshore sites for design of combined wind and wave energy devices. In: 32nd International Conference on Ocean, Offshore and Arctic Engineering Volume 8. Ocean Renewable Energy. American Society of Mechanical Engineers (ASME).
Lydia, M., Kumar, S.S., Selvakumar, A.I., Kumar, G.E.P., 2016. Linear and non-linear autoregressive models for short-term wind speed forecasting. Energy Convers. Manag. 112, 115–124.
Mahjoobi, J., Etemad-Shahidi, A., Kazeminezhad, M., 2008. Hindcasting of wave parameters using different soft computing methods. Appl. Ocean Res. 30 (1), 28–36.
Mahjoobi, J., Mosabbeb, E.A., 2009. Prediction of significant wave height using regressive support vector machines. Ocean. Eng. 36 (5), 339–347.
Malekmohamadi, I., Bazargan-Lari, M.R., Kerachian, R., Nikoo, M.R., Fallahnia, M., 2011. Evaluating the efficacy of SVMs, BNs, ANNs and ANFIS in wave height prediction. Ocean. Eng. 38 (2–3), 487–497.
Mamdani, E.H., 1974. Application of fuzzy algorithms for control of simple dynamic plant. In: Proceedings of the Institution of Electrical Engineers. IET, pp. 1585–1588.
Mandal, S., Rao, S., Raju, D., 2005. Ocean wave parameters estimation using backpropagation neural networks. Mar. Struct. 18 (3), 301–318.
Niu, T., Wang, J., Zhang, K., Du, P., 2018. Multi-step-ahead wind speed forecasting based on optimal feature selection and a modified bat algorithm with the cognition strategy. Renew. Energy 118, 213–229.
Özger, M., Şen, Z., 2007. Prediction of wave parameters by using fuzzy logic approach. Ocean. Eng. 34 (3–4), 460–469.
Poggi, P., Muselli, M., Notton, G., Cristofari, C., Louche, A., 2003. Forecasting and simulating wind speed in Corsica by using an autoregressive model. Energy Convers. Manag. 44 (20), 3177–3196.
Qin, M., Li, Z., Du, Z., 2017. Red tide time series forecasting by combining ARIMA and deep belief network. Knowl. Based Syst. 125, 39–52.
Schlink, U., Tetzlaff, G., 1998. Wind speed forecasting from 1 to 30 minutes. Theor. Appl. Climatol. 60 (1–4), 191–198.
Stefanakos, C., 2016. Fuzzy time series forecasting of nonstationary wind and wave data. Ocean. Eng. 121, 1–12.
Stefanakos, C., 2016. Nonstationary prediction of wind and waves in the Pacific Ocean using fuzzy inference systems. In: The 26th International Ocean and Polar Engineering Conference. International Society of Offshore and Polar Engineers.
Stefanakos, C., Schinas, O., 2015. Fuzzy time series forecasting of bunker prices. WMU J. Marit. Aff. 14 (1), 177–199.
Stefanakos, C.N., Athanassoulis, G., Barstow, S., 2006. Time series modeling of significant wave height in multiple scales, combining various sources of data. J. Geophys. Res.: Oceans 111 (C10).
Stefanakos, C.N., Schinas, O., 2014. Forecasting bunker prices; A nonstationary, multivariate methodology. Transp. Res. C Emerg. Technol. 38, 177–194.
Stefanakos, C.N., Vanem, E., 2018. Nonstationary fuzzy forecasting of wind and wave climate in very long-term scales. J. Ocean Eng. Sci. 3 (2), 144–155.
Sylaios, G., Bouchette, F., Tsihrintzis, V.A., Denamiel, C., 2009. A fuzzy inference system for wind-wave modeling. Ocean. Eng. 36 (17–18), 1358–1365.
Taieb, S.B., Bontempi, G., 2011. Recursive multi-step time series forecasting by perturbing data. In: 2011 IEEE 11th International Conference on Data Mining. IEEE, pp. 695–704.
Takagi, T., Sugeno, M., 1993. Fuzzy Identification of Systems and its Applications to Modeling and Control, Readings in Fuzzy Sets for Intelligent Systems. Elsevier, pp. 387–403.
Tolman, H.L., 1991. A third-generation model for wind waves on slowly varying, unsteady, and inhomogeneous depths and currents. J. Phys. Oceanogr. 21 (6), 782–797.
Torres, J.L., Garcia, A., De Blas, M., De Francisco, A., 2005. Forecast of hourly average wind speed with ARMA models in Navarre (Spain). Sol. Energy 79 (1), 65–77.
Veritas, D.N., 2011. DNV-OS-H101. Marine Operations, General. DNV Offshore Standards (OS) H; DNV: Oslo, Norway 101.
Wang, C., Zhang, H., Fan, W., Fan, X., 2016. A new wind power prediction method based on chaotic theory and Bernstein Neural Network. Energy 117, 259–271.
Watson, S., Landberg, L., Halliday, J., 1994. Application of wind speed forecasting to the integration of wind energy into a large scale power system. IEE Proc. Gener. Transm. Distrib. 141 (4), 357–362.
Wilson, B.W., 1965. Numerical prediction of ocean waves in the North Atlantic for december, 1959. Deutsche Hydrografische Zeitschrift 18 (3), 114–130.
Zuluaga, C.D., Alvarez, M.A., Giraldo, E., 2015. Short-term wind speed prediction based on robust Kalman filtering: an experimental comparison. Appl. Energy 156, 321–330.